The referee comments are italicized. Answers in regular typeface. Actions taken in red.

Answers to referee 1 comments

Anonymous Referee #1:
Summary: The paper by Parvathi et al. investigates the seasonal and interannual variability of dissolved oxygen off the West Coast of India (WCI) using a coupled physical-biogeochemical regional simulation of the North Indian Ocean. More specifically, the study documents the recent variability in the oxycline along the WCI and explores its potential drivers. It is shown that the seasonal as well as the year-to-year fluctuations in the depth of hypoxia (and hence the likelihood of occurrence of anoxic events in the near-surface coastal waters) are controlled to a large extent by the variability of the depth of the thermocline, and hence are essentially physically driven. Authors show that oxycline like thermocline is shallowest in fall, thus eventually allowing anoxia to develop and reach the coastal region during this period of the year. Finally, it is shown that the year-to-year fluctuations in the oxycline (and hence the potential severity of hypoxia) in the WCI region is partially controlled by the Indian Ocean Dipole (IOD). This is because of the sensitivity of the thermocline in this region to coastal Kelvin waves generated by easterly wind anomalies associated with IOD. Yet this effect is only strong during positive IODs where the downwelling Kelvin waves generated by easterlies near the southern tip of India lead to a deepening of the oxycline that prevents anoxia. In contrast, during negative IODs the effect is of smaller amplitude and hence is less important. The authors conclude that these findings have important implications in terms of the predictability of fall anoxia along WCI.

General comment:
The subject of the paper is highly relevant in the general context of quantifying and better understanding the drivers of naturally occurring coastal anoxia and what controls its year-to-year variability. The paper is well written and presents important new findings. The experimental design is appropriate despite some limitations (e.g., model resolution). For these reasons I recommend the publication of this manuscript after improving the presentation and the discussion of certain aspects of the study, namely the potential role of biology in contributing to O2 variability and the implications of the model low-resolution for the conclusions of the study.

We thank the referee for his encouraging review. As detailed below, we propose to improve the presentation and discussion of the potential role of biology in contributing to O2 variability and the implication of the low-resolution of the model used.

Here below I detail my comments:
Specific comments:
Page 2, line 16: "The frequent anoxic conditions that occurred…"

This has been corrected.

Page 4, line 13: The 1/4 horizontal resolution does not allow a proper representation of coastal upwelling either. The underestimation or potential misrepresentation of coastal (wind-driven) upwelling in the model needs to be mentioned and its potential implications discussed.

We briefly mention this model limitation in the introduction section but defer to the discussion section for more extensive discussion regarding the implications of the underestimation of coastal upwelling. The discussion on the model limitation has been considerably expanded and can now be found in the last section of the manuscript (see from P17 L18 to P18 L14).

Page 5, lines 9-20: in addition to the limitations discussed by authors, the CaTS dataset comes from a single coastal site and hence may not be representative of the dynamics of the whole WCI. This needs to be stressed.

The referee comments are italicized. Answers in regular typeface. Actions taken in red.

Thank you for pointing this out. This is now mentioned in the revised draft (P5, L22-23).

Page 6, 2nd equation: all parameters ($R^1_{o:c}$, $R^2_{o:c}$, etc…) should be explicitly defined in the text.

All parameters are now explicitly defined in the revised draft (P6 L22-26).

Page 6, Is sediment respiration represented in the model? Please specify. Also, how are denitrification and anamox represented in the model?

We agree with the reviewer that such a description was missing in the earlier version of the paper. The model indeed includes a very simple description of the sediment processes. The metamodel of Middelburg et al. (1996) is also used to compute the relative contribution of denitrification to the remineralization of the organic matter. Denitrification starts when oxygen falls below a threshold set to 6 µmol.L^{-1}: below this threshold, nitrate instead of oxygen starts to be increasingly consumed during the remineralization of organic matter. However, anamox is not represented in the model. To address the reviewer comment, a more thorough discussion of these modelling aspects have been included in the model description section of the paper (P6 L27 to P7 L4).

Related reference:

Middelburg, J. J., Soetaert, K., Herman, P. M., & Heip, C. H.: Denitrification in marine sediments: A model study. *Global Biogeochemical Cycles*, *10*(4), 661-673, 1996.

Page 9, lines 14-15: I don't think the effect of biology on oxygen is small at the thermocline depth. The respiration fluxes can be very large at 100m. The fact that the oxycline and the thermocline show high correlations may result from the fact that biology itself is constrained by vertical physics and as a consequence that the nutricline and the thermocline are tightly coupled. This statement needs to be reformulated and the role of biology further discussed (authors may consider quantifying the individual contributions of biology and physical transport to oxygen variability).

Resplandy et al. (2012) did already quantify the respective contributions of biology and vertical transport to the seasonal oxygen variability along the west coast of India. Despite the compensation of biological sink and dynamical source of oxygen on an annual average, they found that the seasonality in the dynamical transport of oxygen is 3 to 5 times larger than that in the biological sink. The seasonality in oxygen along the WCI hence primarily arises from the vertical displacement of the oxycline attributed to the influence of northward propagating coastal Kelvin waves forced remotely from the Bay of Bengal. This conclusion does not support the hypothesis of Sarma (2002), who suggested that the weak oxygen seasonality could arise from compensation between the dynamical input and the biological uptake of oxygen during each season. This hypothesis could not however be verified owing to the absence of reliable seasonal estimates of oxygen consumption (Sarma, 2002). The text has been modified to explicitly mention the dominance of vertical transport on the modelled seasonal oxygen variations in this region derived from the oxygen budget analysis of Resplandy et al. (2012) (see P10 L4-13).

Related references:

Resplandy, L., Lévy, M., Bopp, L., Echevin, V., Pous, S., Sarma, V. V. S. S., and Kumar, D.: Controlling factors of the oxygen balance in the Arabian Sea's OMZ, Biogeosciences, 9, 5095–5109, doi:10.5194/bg-9-5095-2012, 2012.

Sarma, V. V. S. S.: An evaluation of physical and biogeochemical processes regulating perennial suboxic conditions in the water column of the Arabian Sea, Global Biogeochem. Cy., 16, 1082, doi:10.1029/2001GB001461, 2002.

Page 9, lines 18-22: It is not clear why the correlation between the OCD and the TCD is low in the southern and the southwestern parts of the domain. In the southwestern part authors mention a

possible role of lateral advection there, but it is not clear how this might affect the correlation between these two quantities.

If any other process than vertical advection strongly contributes to OCD variability (i.e. lateral advection, biology, etc…), there is no reason for OCD variability to be in phase with TCD variability and correlation between the two variables should hence decrease.

In the equatorial region authors suggest the low correlation may be due to the definitions used for oxycline and thermocline that may not be meaningful there. Yet, in section 2.4 (page 8, lines 28-31) it is stated that the results and the conclusions of the study are insensitive to the oxygen (50-150 mmol/m3) and temperature (20-25C) criteria used to define these two depths. These two statements appear to contradict each other.

We agree that these two statements are misleading. We meant that main results regarding the variability of the OCD/TCD variations in the Arabian Sea and more specifically in our focus region along the WCI are not sensitive to that choice. This has been clarified in the revised manuscript that this holds for the northern Indian Ocean only (P9 L13-16).

Page 9, lines 25-27: during the spring inter-monsoon, the (northwesterly) winds along the WCI are also upwelling-favorable. Yet, the thermocline is relatively deep there (especially in observations). This is an indication that TCD alone cannot be used as a proxy for wind-driven coastal upwelling (probably because of the non-local effects of the coastal Kelvin waves).

We agree with the reviewer. This is now mentioned in the revised manuscript (P10 L23-26).

Page 10, lines 4-5: in the northern part of the WCI, alongshore (southward) winds seem to be upwelling-favourable. Maybe plotting seasonal time series of upwelling index together with OCD and TCD would help figuring out how these three quantities co-vary (can be added to Fig 7).

Following the reviewer concern, the paper has been revised to include a more thorough discussion of the local and remote wind control on the OCD and TCD variations along the west coast of India. The updated Figure 7 now provides a direct comparison between the wind seasonal variations along the coast and at the southern tip of India and the west coast of India oxygen seasonal variability in both the model and observations. This figure shows that the TCD starts to shallow in April and becomes shallowest in September-October, the peak season of the upwelling. Local alongshore winds along the WCI are favourable to upwelling only during the southwest monsoon, indicating the influence of remote wind forcing on the upwelling along the WCI. The text has been accordingly revised to describe this feature in more detail (P11 L10-30).

Page 10, lines 24-32: the overestimation of oxygen in the WCI may not only be due to the coarse representation of the shelf dynamics but also the general tendency of the model to underestimate the intensity of the OMZ in the northern Arabian Sea (see Fig 4 for example). This needs to be discussed.

We don't necessarily agree with that statement. The good agreement between the model and WOA seasonal oxygen variations in the WCI box (Fig. 7) suggests that the model is able to accurately capture the oxygen variations offshore the WCI. This good agreement suggests that the model OMZ underestimation in the northwestern AS (Fig. 3ac) does not affect the oxygen representation along the WCI. It is hence more likely that shelf-specific processes may explain the lower oxygen contents observed at CaTS as compared to the model and WOA data. These issues are in any case now addressed in the discussion section (P18 L1-14).

Page 13, lines 7-8: Identifying the drivers of coastal anoxia requires further investigation. In particular, the role of biology and the effects of O2 consumption on the shelf need to be quantified and contrasted with the impact of vertical and lateral advection. It is not clear how much of anoxia is driven by large-scale advection of O2-depleted water (from the Arabian Sea OMZ) vs. local

The referee comments are italicized. Answers in regular typeface. Actions taken in red.

consumption of O2 due to respiration in the water column and on the shelf.

We agree with the reviewer that this statement is too strong, given our model limitations. We tuned down that statement in the revised manuscript (P15 L7-8). In addition, a revised discussion on the need of a refined assessment of the large-scale and local biological processes influencing anoxia along the shelf is now provided in the discussion section (from P17 L29 to P18 L14).

Page 13, lines 17-20: Any explanation for the asymmetry of the impacts of positive and negative IODs (and in particular the potential reason for why the wind anomalies are weaker during negative IODs)?

Negative IODs tend to be weaker than their positive counterpart due to nonlinear response of the deep atmospheric convection to SST anomalies (Saji and Yamagata 2003; Hong et al. 2008; Cai et al. 2013). The differences in wind patterns (the fact that for a given DMI absolute value, positive IODs tend to display wind anomalies that extend more northward) may also be related to this asymmetry. This is now mentioned in the revised manuscript (P16 L9-16).

Related references:

Cai, W., Zheng, X. T., Weller, E., Collins, M., Cowan, T., Lengaigne, M., ... & Yamagata, T. (2013). Projected response of the Indian Ocean Dipole to greenhouse warming. *Nature Geoscience*, *6*(12), 999-1007.

Hong, C. C., Li, T., & Kug, J. S. (2008). Asymmetry of the Indian Ocean Dipole. Part I: Observational Analysis*. *Journal of climate*, *21*(18), 4834-4848.

Saji, N. H., & Yamagata, T. (2003). Possible impacts of Indian Ocean dipole mode events on global climate. *Climate Research*, *25*(2), 151-169.

Page 15, lines 11-14: As acknowledged by the authors, the (relatively) coarse resolution of the model (1/4) is probably the main limitation of the study. The underestimated or misrepresented coastal upwelling and mesoscale eddies in the model may have important consequences. I encourage the authors to further discuss the implications this might have and how it may (or may not) affect their conclusions/results

This has been done in the revised discussion (cf answers to your first comment).

Page 15, lines 11-16: if the model does not represent sediment processes, the lack of benthic respiration could also limit the model ability to represent the dynamics of coastal hypoxia along the shelf. This needs to be clarified.

The model does include a simple representation of sediment processes. The simplicity of this representation may however be a limit of the model's ability to represent the dynamics of coastal hypoxia. This will be clearly stated in the updated discussion of the potential role of biology that is quoted in answer to your comment above (from P17 L29 to P18 L14).

Figure 3: the colorbar is missing.

Sorry for this. Thank you for pointing this out. The colorbar has been added.

Figure 3: since the study focus is on coastal anoxia that develops during fall, maybe it would be good to show how the model reproduces chlorophyll during this season.

Figure R1 below provides the summer and fall Chl patterns for the model and observations. As shown in this Figure, the patterns during these two seasons share a lot in common, with a tendency for weaker Chl values in fall compared to summer in both model and observations. We hence did not

include the fall Chl pattern in the revised manuscript but will clearly state that the fall Chl patterns are similar, although weaker, than those in summer in both observations and model (P8 L25-26).

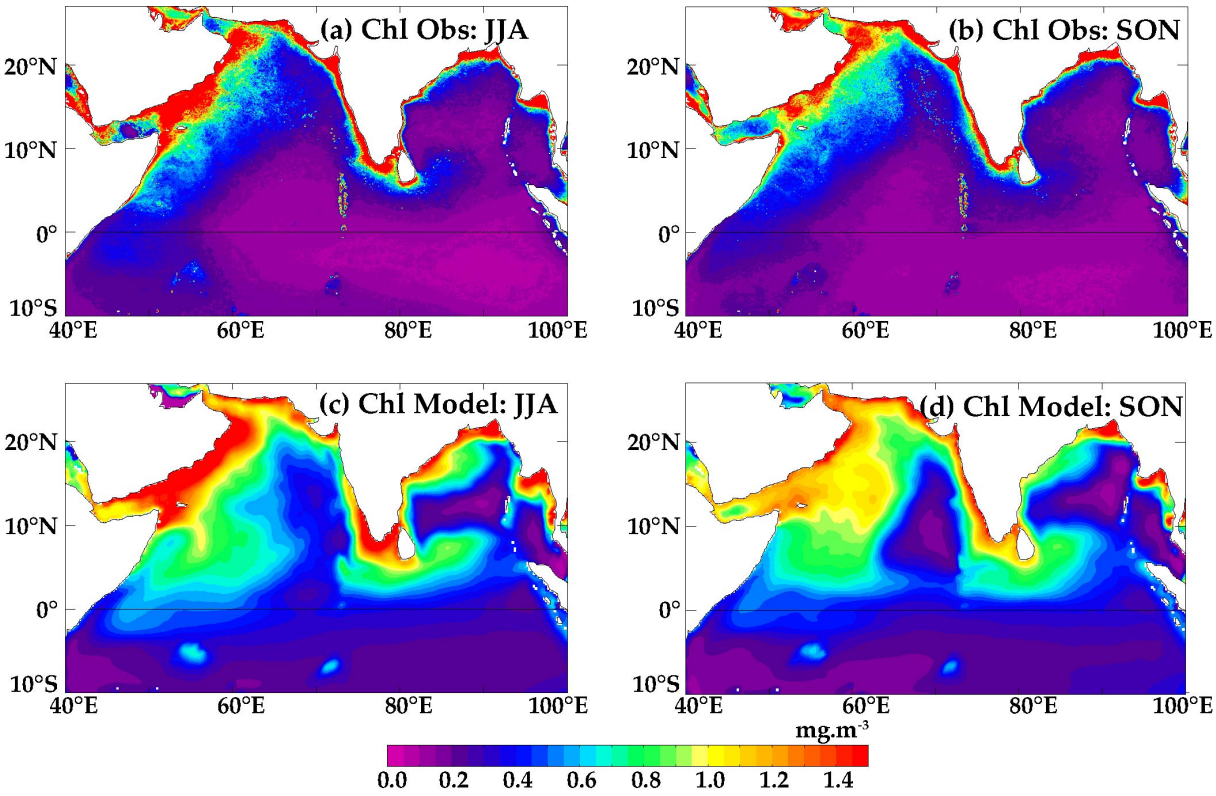

Figure R1: Northern Indian Ocean surface chlorophyll (mg.m^{-3}) climatology for (left) summer (June-August) and (right) fall (September-October) in (top) the ESA satellite product and (bottom) model.

The referee comments are italicized. Answers in regular typeface. Actions taken in red.

Answers to referee 2 comments

General comments: Ultimately, I think that there could be a linkage whereby positive IOD occurrence influences OCD conditions along the SW coast of India. The authors have taken a great stab at establishing this link but have fallen a bit short, in my opinion, of establishing the case. Significantly tightening up the analysis, following the suggestions I have made in specific comments below, would go a long way toward achieving a reasoned, well considered analysis that can at least strongly suggest such a linkage is present. It may be that additional data, refinement of this analysis in terms of key locations for exploring causality and higher resolution modeling with nested shelf regions, will be required to fully reveal what is tantalizingly indicated in the current effort.

We thank the reviewer for his encouraging comments. We followed all reviewer's suggestions, which led to significant changes in the Figures list as summarized below:

1- As suggested by the reviewer, results from Figure 1 have been integrated in the new Figures 6 and 7. The text related to the earlier figure has hence been dropped from the introduction and a more precise discussion on the past literature discussing the offshore/shelf oxygen connection is now included in the introduction.

2- New Figure 4 provides a comparison between O2 and temperature seasonal variations in the WCI box for both model and WOA data.

3- The updated Figure 7 gathers results from old Figure 7 augmented with an assessment of local and remote (from the southern tip of India) seasonal wind variations. This updated Figure allows us discussing in more details: (1) the modelled and observed seasonal phasing between upwelling and oxygen depletion, pointing towards a strong physical control of seasonal oxygen variations, (2) the seasonal phasing between offshore and coastal oxygen variations, further highlighting the offshore/coastal connection at seasonal timescales and (3) the remote influence of STI wind seasonal variations on WCI upwelling variability.

4- The updated Figure 8 now includes timeseries of interannual oxycline and thermocline variations in the WCI box, further highlighting their in-phase relationship and hence the strong physical control onto WCI interannual oxycline variability.

5- The updated Figure 9 allows demonstrating the strong control of STI wind variability on observed and modelled WCI interannual thermocline variations through coastal Kelvin waves, along with the ability of the model to capture observed interannual thermocline variations in the WCI region.

6- The updated Figure 10 is a simplified version of previous Figure 10, from where the correlation between winds and the WCI oxycline / DMI index has been removed.

7- The updated Figure 11 demonstrates that (1) WCI interannual OCD variations are well correlated to the DMI index computed from either the model and observations and (2) that these variations are remotely controlled by interannual wind variations in the STI region rather than by local winds.

These new figures are appended below for your reference and the text will be changed accordingly. Below, we further provide point-by-point answer to each of your specific concerns.

Specific comments :

The referee comments are italicized. Answers in regular typeface. Actions taken in red.

Introduction, p. 2 & 3. The bottom paragraph of p. 2 and top paragraph of p. 3 have diverted from providing background information of the research to be undertaken to an initial summarizing, drawn from figure 1, of aspects of the study that is being reported on. This leads to an awkward shifting between presenting problem framework and results that interferes with coherent, logically developed reporting. I would recommend that all call outs to Fig. 1 be eliminated from the Introduction section. This could be simply accomplished by shifting the two noted paragraphs out, but note that there is at least one additional callout to Fig. 1 to address. As to the content of these two paragraphs, I do have additional specific comments. In the first of these paragraphs, the authors first introduce the notion that the open ocean OMZ of the Arabian Sea has connectivity to the hypoxia that manifests along the west coast of India. From my knowledge of the literature, and from the literature the authors' have cited, this has so far only been posited and in my view is more anecdotal than proven fact. The 1/4_ model solution that the authors use as principal basis of their findings is challenged to demonstrate causality on this point. The authors should acknowledge this explicitly, make a more compelling case based on existing literature, or leverage this in from some of their higher resolution modelling efforts.

The seminal paper by Banse (1959) shows a section across the shelf off Cochin located ~10°N on the west coast of India. Based on the analysis of this section, Banse (1959) stated that the hypoxic conditions off Cochin were clearly connected with seasonal upwelling variations in relation with the southwest monsoon. Similar findings were reported off Bombay by Carruthers et al. (1959), who showed the layer of minimum oxygen was upsloping towards the coast right after the summer monsoon demise. Similar cross-shore sections along the west coast of India across the monsoon season are shown in Naqvi et al. (2009) and used to support the notion that it is the seasonal upwelling that brings to the west Indian continental shelf the oxygen-poor subsurface waters that then turn anoxic by late summer due to exhaustion of oxygen and nitrate by heterotrophic micro-organisms. Another recent paper (Gupta et al. 2016) further concluded that upwelling of oxygen-deficient waters during the monsoon is the major process regulating the biogeochemistry along this shelf using ten shelf transects during 2012 near 10°N. We believe that these observational analyses at different locations along the west coast of India are clear indications that there is some connection between open ocean seasonal oxygen variability and coastal hypoxia. We however agree with the reviewer that the discussion based on Figure 1 should rather belong to the result section. We also agree with the reviewer that the detailed processes by which these exchanges occur are not yet properly understood, nor resolved by our model or existing datasets. To address the reviewer's concerns, we have performed the following changes:

1- All callouts to Figure 1 has eliminated from the introduction. Results from this Figure has been incorporated in Figures 6 and 7 to discuss the connection between the offshore and costal seasonal O2 variability and the role of the remote and local seasonal alongshore wind variations in driving this variability in more detail.

2- We have rewritten the bottom paragraph of p2, to more precisely acknowledge on which observational basis the influence of upwelling has been reported as the major process driving the coastal hypoxia along the West Indian continental shelf. We especially refer to the results of Banse et al. (1959), Carruthers et al. (1959), Naqvi et al. (2009) and Gupta et al. (2016) who all support this offshore-coastal connection based on the analysis of the cross-shore transects data at different locations along the west coast of India. We however also clearly acknowledge in this paragraph that these conclusions were drawn from punctual cruises snapshots and that the processes through which these exchanges take place are unclear. Updated Figure 7 now provides a comparison of the seasonal oxygen evolution offshore and at the coast and of the remote and local alongshore winds. It allows clearly illustrating the strong seasonal phasing between the offshore and coastal evolution, further pointing towards a strong connection between open ocean OMZ and coastal hypoxia through the upwelling processes. This Figure also allows to demonstrate the remote control of the alongshore winds at the southern tip of India on the seasonal upwelling conditions along the west coast of India.

3- We have also clarify when introducing the model that it does not resolve the details of the

The referee comments are italicized. Answers in regular typeface. Actions taken in red.

shelf / open ocean interactions, but is merely used to understand the processes that control offshore variations (P4 L14-18). We have also included a discussion of the need for improved observations and modeling to resolve processes of shelf-open ocean exchanges in the discussion (P17 L17 to P18 L22).

Page 5, line 20. In the last sentence, it is interesting to note that these observed instances of full anoxia will be featured/discussed later in the paper but the figure callout should not be included. Could probably accomplish this through merging of that point into the prior sentence and eliminating the remainder.

We removed the callout to the figure in the revised version as suggested.

Page 6, line 8. In this equation describing the biological source / sink terms of DO, it would be interesting to note what is done to ensure negative concentrations of dissolved oxygen are not achieved in the model.

There is a specific treatment that allows model not to reach negative values by switching off all processes consuming O2 below a 10^{-3} µmol.L^{-1} threshold. This is now mentioned in the updated manuscript (P6 L27-28).

Page 9, lines 1-2. The text here is a bit confusing. At the top of the paragraph it is stated: "… we used the standard Dipole Mode Index …". From the subsequent text in this section that indicates DMI based on model SST is calculated, I think what is meant is " … the standard DEFINITION of Dipole Mode Index …" is used.

Corrected. We have now provided correlations with the DMI derived both from the model and the observations.

Page 9, line 6. " to the choice of either of them" is awkward. "which is chosen" would work better.

This sentence has been modified, thanks.

Page 9, line 26 -> top page 10. In the model during MAM, Fig. 6e shows that OCD is not really uniform in eastern AS; and OCD off Mumbai is comparable in value to OCD at bottom of the subcontinent. This directly contrasts what is described in the text. It also dampens the scenario described as a clear-cut influence of coastal KW propagation northward of the shoaled OCD / TCD condition that initiates in the STI region. I believe that the issue here is that care needs to be taken to make clear that description is centered on WCI to STI region and not relevant north of 10° where alongshore wind forcing is distinct from what exists farther south.

To address the reviewer comment, this description has been improved (P10 L22-27).

Page 10, line 8. I think it is stretching what can be elucidated from the model results and presented figures to say that the OCD/TCD pattern is clearly suggestive of faster planetary wave propagation at lower latitudes. Lag associated with coastal KW propagating northward could also factor in.

We agree. This is now mentioned in the updated version (P11 L1-2).

The referee comments are italicized. Answers in regular typeface. Actions taken in red.

Page 10, bottom paragraph. The linkage of offshore OMZ to low coastal DO is again a thread in this part of text (see earlier remarks on my reservations).

This discussion has been considerably strengthened in the updated manuscript by following the reviewer's suggestion (see P11 L10-29). Figure 7 now provides a comparison of the seasonal oxygen evolution offshore and at the coast and of the remote and local alongshore winds. It shows that oxygen seasonal variations along the coast from CaTS in-situ measurements match the corresponding offshore variability derived from the WOA and model data, suggesting a strong connection between the two. The seasonal wind evolution further allows discussing the respective influences of local and remote forcing (from the southern tip of India) in driving these variations.

Page 11, lines 3 - 17, and figure 9. There are a number of interesting features in figure 9. Some comment on the inverse correlation regions appearing in 9a would be interesting to include and may provide some mechanistic insight to IOD-associated biophysical interaction that is the crux of this analysis. Some comment on the several instances where model TCD and observed SLA are out of phase in the 2002-2006 period (9b) would also be potentially illuminating (model issue?, sensitivity to WCI box definition?). Assessing any limitations in either of these is key to explore and characterize for the reader to fully trust results stemming from this analysis.

This figure and the related text has been revised in the updated version to better discuss the physical mechanisms driving the interannual variations along the west coast of India (from P12 L15 to P13 L10). Figure 9 is split into two separate Figures (new Figure 8 and 9). The new Figure 8 now includes previous Figure 9a along with timeseries of interannual TCD and OCD variations in the WCI box, to further highlight the strong physical control of interannual oxygen variations in this region. The new Figure 9 now includes previous Figure 9b augmented with time series wind variations at the southern tip of India and two additional maps. The new Figure 9b displays the correlation pattern of interannual model TCD in the northern Indian Ocean onto the timeseries of fall model TCD in the WCI box. New Figure 9c shows a similar analysis but for observed SLA. This Figure allows highlighting the good match between the interannual thermocline variations along the WCI. The good match between timeseries of interannual wind fluctuations at the southern tip of India provided on Figure 9a and both WCI modelled TCD and observed SLA (-0.65 and -0.69 correlation respectively) further demonstrates the role of remote wind fluctuations at the southern tip in driving the west coast interannual variations through coastal Kelvin wave propagation. Despite the generally very accurate model behavior, we also mention the periods where the model agreement is weaker (2002-2006). Finally, the TCD and SLA patterns shown on Figure 9bc are also reminiscent of the typical IOD pattern. The relationship with IOD is further illustrated on Figures 10 and 11.

Page 11, lines 19-20. Details of how anomalies are determined would be useful to document; caption of Fig. 10 is an option if this is not substantial enough to stand alone in methods section. Also, on line 20 panels a-c are noted as regression maps, which is contradictory to the information in the Fig. 10 caption (and plot labeling) that states panel c is a correlation map. For both of these data reductions details of how they are performed are not documented, making it problematic for the reader to correctly self-determine his/her interpretation. As for grasping why distinct analysis method was to zonal wind stress relative to how the other variables (OCD, TCD, SST) were treated, that is even more of a challenge for the reader to intuit.

Interannual anomalies for all variables have been calculated from monthly time-series by subtracting the mean seasonal cycle and applying a 3-month smoothing to remove the sub-seasonal variations. This has been explicitly stated in the Data and Method section (P9 L19-20). The panel with correlations is indeed confusing and anyway not necessary: we removed it and provided the regressed wind stress anomalies on panel a.

The referee comments are italicized. Answers in regular typeface. Actions taken in red.

Page 11, lines 19 - 23 and caption for Fig. 10. The terminology used in referring to the derived fields described here, and the terminology in the captions that accompany the associated distributions in Fig. 10, is inconsistent. Specifically, the narrative notes that all variables are internally varying anomalies but in the caption this is not obvious. In the caption, the data shown in panels a-c are noted to be regressed against "normalized oxycline interannual anomalies averaged over WCI box". My interpretation is that this describes the ts shown in Fig. 11a. If this is indeed the case, noting that as such would be very helpful to the reader as a way to better grasp what is presented in Fig. 10. This may entail modifying figure ordering w/in the ms.

First, we agree that the terminology used in the caption of Figure 10 and in the related text were inconsistent. The bottom panels with correlations have been removed and regressed wind stress anomalies have been added on top panels. In addition, the WCI OCD time series used to obtain the regression maps shown on Figure 10 is now plotted in Figure 8b. This is now clearly stated both in the modified text and in the caption of Figure 10.

I find it interesting that the regression of OCD with OCD(WCI) in the WCI box (panel 10a) is actually relatively low compared to elsewhere in the IO domain. I think some interpretive commentary from the authors would be very interesting to see. Further, as I questioned earlier, does this have implications for the sensitivity / utility / robustness of the WCI box as a foundational component of this analysis? I would like to see the authors critically assess and comment on the choices they have made in setting up and carrying out their analysis.

We first added a couple of additional sentences to explain more clearly the meaning of these regression maps, i.e. that they provide the basin scale typical anomalies corresponding to an anomalously deep OCD in the WCI, which are indeed similar to those associated with a high DMI, i.e. a positive IOD (P13 L12-14). It is true that the regression coefficients of OCD in the WCI box are rather low (~6 m) as compared to the eastern equatorial Indian Ocean (~15m). This reflects the fact that the amplitudes of interannual OCD/TCD fluctuations are generally weaker in this region compared to other places. However, these small fluctuations have a tremendous impact on the ecosystem and related fisheries and hence deserve to be better understood. It must be noticed that, despite the modest WCI regression coefficient, corresponding correlation coefficients from this region to the southern tip of India are very large (see Figure 9bc), demonstrating that the variability in the WCI box is representative of the OCD/TCD variations all along the western and southern coasts of India. The main conclusions of the paper do not change for a slightly different choice of the boundaries of the WCI box, as now noted when introducing this box (P9 L18-19).

Page 11, line 24. For clarity and to benefit the reader, please explicitly associate / define how shallower / deeper OCD anomaly relates to + / - OCD anomaly.

This will be clarified (P13 L16, L18).

Page 11, lines 25-31. The KW propagation patterns noted here are consistent with what is reported in the literature. However, the pathways and timings that are discussed are not identifiable in the Fig. 10. Appropriate referencing of the literature should be given to support what is stated. The remote forcing aspect of thermocline dynamics in the northern IO is quite complex; I strongly encourage the authors to make the effort to clearly articulate and document what is known and how it relates to their study. I believe this would be highly appreciated by the IO readership.

Appropriate referencing of the literature are now provided in this paragraph (P13 L12-30).

Page 11, line 31. Should specify that the correlation referred to here is negative.

The referee comments are italicized. Answers in regular typeface. Actions taken in red.

Done.

Page 12, lines 4-8. The correlation distribution pattern for taux (Fig. 10c) is different enough that I would hesitate to even characterize it as "reminiscent of IOD signature"; in particular the sign shift in correlation that is apparent in the NE Bay of Bengal and eastward / off equator shift of strongest correlation (i.e., away from Sumatra coast where + IOD signature is most pronounced). Note as well that this is positive IOD signature. And related to that call for clarification, it would be nice to include an example of negative IOD manifestation to accompany the example of positive IOD (Fig. 5d).

Earlier figure 10c has been removed (cf earlier comment). Several diagnostics in the paper point towards an influence of IOD on OCD/TCD variations in the WCI: (1) basin-scale wind stress patterns associated with anomalous OCD along the west coast of India (now on upper panels of updated Figure 10) look very similar to those associated with the DMI (i.e. a way to estimate the IOD wind signature), and we now state that the the OCD pattern correlation is 0.85, (2) the new correlation patterns provided in Figure 9bc also resemble the IOD signature on thermocline and SLA variability and (3) both observed and model-derived DMI correlate well (0.62 and 0.67) with WCI interannual OCD variations. We thus think that we can state that this pattern is "reminiscent of the positive IOD signature". The asymmetries between positive and negative IODs are explicitly discussed later in the text based on Figure 13.

Page 12, line 6. Here, the 10 d-f sequence is collectively referred to as regression maps, which is inconsistent with labeling / reporting elsewhere in narrative.

The modifications in the figures of the revised version address this point.

Page 12, lines 8-9. I think it is a stretch to make the statement that these figures, in particular panel 10d which is the key for illustrating the point, demonstrate a "strong link" between OCD in WCI region and IOD. In my view the level of regression in 10d for the WCI region is marginal and certainly much less pronounced than elsewhere (e.g., the Sri Lanka Dome).

The "strong" was indeed a too "strong" word. We now explicitly state the 0.62/0.67 correlation between OCD in the WCI region and the observed/model DMI, and state that it is significant at the 99% level. More explicitly, we now explain that basin scale OCD, TCD and wind stress patterns associated with OCD anomalies in the WCI region look very similar (and we now mention pattern correlations to support this) to those associated with the IOD (i.e. obtained through a regression with the DMI). This clearly supports the link we mention, although we agree it was not explained clearly enough in the previous version of the manuscript. The level of regression of Fig. 10d is an indication of the amplitude of the signal related with the IOD (which is of course stronger in the equatorial region) but does not provide direct information about how much the IOD control the variability there. Correlation provides this kind of information (the correlation squared being the level of OCD/TCD variance explained by the IOD).

Page 12, lines 10-11. The correlation between model-based DMI and OCD(WCI) is interesting and suggestive of what the authors are trying to demonstrate (i.e., causal link between OCD and DMI). I would strongly suggest that this correlation also be performed with standard DMI product, for a couple of reasons. While the authors did report earlier in the ms that the standard DMI and their model-based DMI were largely similar and choice of which is applied did not substantially affect the results, performing the correlation with standard DMI provides grounding to a well-known established index and would mitigate any concerns that may/should arise for the reader vis a vis internal bias inherent in a model-model comparison.

We now provide a comparison of the WCI OCD interannual variability with both model and observed DMI on this Figure. Because the observed and model DMI are strongly correlated (0.94), OCD interannual timeseries correlate well with both model DMI (0.67 correlation) and observed DMI (0.62). This is now discussed in the updated manuscript (P14 L5-9). To further strengthen the physical

The referee comments are italicized. Answers in regular typeface. Actions taken in red.

explanation of how the IOD can influence the OCD variations along the WCI, Figure 11bc also provide the timeseries of the local and remote alongshore wind stress forcing: this analysis clearly shows that the interannual OCD variations along the WCI are far more correlated with STI winds (-0.73) than with local alongshore winds (-0.25). This now discussed in the revised text (P13 L27-29).

Page 12, lines 14-21, and Fig. 11b. This is an interesting distillation of results, though I still have reservations of robustness similar and related to what has been noted in comments above. I think it would be useful to find a way to split out the DMI values such that those that pass threshold and can be classified as positive / negative IOD are distinct from those that do not (i.e., normal and IOD states are clearly delineated). The regressions that are shown do not add much insight, but if they are retained then they should be performed only on points that are +/- IOD states and not inclusive of all positive of negative values.

The updated Figure 12 (previous Fig. 11b) now highlights with different color codes the years corresponding to positive and negative IOD events (red and blue dots respectively) along with neutral years (black dots). Positive (resp. negative) IOD events are identified as years when the DMI index exceeds one standard deviation (resp. is lesser than minus one standard deviation). All other years are classified as normal years. Regression lines have been removed from the revised manuscript, as they did not provide much insight, as pointed out by the reviewer.

However, even doing this, I am skeptical that particularly insightful result will be obtained. For the data that are shown that do represent + /- IOD occurrence, there is not really an associated systematic deepening / shoaling of OCD. Certainly the negative IOD case has a number of either OCD result. But there is also a positive IOD case with (slightly) shallowing OCD. It also appears that the years with observed and notable anoxic events tend to be during negative DMI (thought not necessarily negative IOD) but there is also a positive DMI case and a case that is almost uniformly normal (i.e., DMI _ 0 and OCD _ 0). Given these results, I do consider that the data are suggestive of positive IOD events influencing appearance of low oxygen in WCI but would be hesitant to make categorical conclusions. Overall, I think the authors need to be more even handed when reporting what is revealed in Fig.11b.

New figure 13 (old Figure 12) clearly demonstrates that, on an average, positive IOD events lead to a deepening of the TCD/OCD along the west coast of India. Similarly, negative IOD events are associated, in general, with a shoaling of TCD/OCD along the WCI. However, although the correlation between DMI and WCI OCD is significant (0.67), it is not close to one, demonstrating that there are clear departures from this average picture. This is actually what is shown on new Figure 12 (previous Figure 11b), where positive IOD can be related sometimes with insignificant OCD anomalies and negative IOD can even be related in some instances with OCD deepening. This suggests that IOD is not the only process that controls the interannual OCD variations along the WCI. Other processes, such as local wind fluctuations or biological processes can indeed counteract the IOD influence. This discussion has been expanded in the revised text (P14 L14-28) and further discussed in the last section. We now clearly state in the abstract that positive IODs suppress favorable conditions for anoxic events along the WCI and negative or neutral IODs are a necessary but not sufficient condition for anoxia to occur along the WCI (P1 L18-24)

Page 12, lines 21-27, and Fig. 12. This figure is also quite interesting. It suggests that both IOD phases lead to positive OCD and TCD displacement during SON, although for negative IOD this may not be statistically significant. What I find curious is that taux during SON in STI that has opposite sign between positive and negative IOD. Would this not lead to opposite oceanic response (i.e., upwelling vs. downwelling) between the two IOD phases, which then presumably has contrasting impact on thermocline displacement if this response translates northwards as coastal KW as authors have argued? The authors do note that taux condition for negative IOD is not as "robust" as that for positive IOD, however the relative values of anomaly for October (highest magnitude for SON period) are not strikingly distinct. Which begs the question as to how much OCD / TCD response one can

The referee comments are italicized. Answers in regular typeface. Actions taken in red.

ascribe to STI wind stress condition.

First, we believe that there is a misunderstanding here. In this Figure, the negative IOD composite time series has been multiplied by minus one to ease comparison with positive events (as stated in the Figure caption). Hence, positive IOD events are associated with OCD and TCD deepening and negative zonal wind stress anomalies at the STI. In contrast, negative IOD events are associated with OCD/TCD shoaling (although hardly significant) and positive zonal wind stress anomalies at the STI. These evolutions are hence consistent with a Kelvin wave response at the STI to zonal wind variations associated with the IOD fluctuations. To avoid confusion, we now mention explicitly in the main text (P14 L21-22), figure caption and figure label (« -1 x Negative-IOD ») that the the negative IOD composite time series has been multiplied by minus one to ease comparison with positive events. To better asses how much OCD response can be ascribed to STI wind stresss variations, the new Figure 11b compares interannual time series of WCI OCD and STI Taux: these two parameters display a strong and significant correlation (-0.73), demonstrating that more than 50% of the OCD variability along the WCI can be attributed to STI wind variations. This will be more clearly stated in the updated text (e.g. P13 L27-29).

Page 12, slide 30. Instead of "identified fifteen years ago", reiterating citation of relevant source material would be best.

This has been done.

Page 20, line 8. Title for this reference is incorrect.

This has been corrected.

Comments on Figures
General comment. There are several figures that include isolines superimposed on a second variable where a color scale is applied. In almost all cases, there is a need for additional labeling of the superimposed contour lines on the plot so these distributions can be grasped. There is also a need to note the contour intervals in the associated captions.

This has been done.

Figure 4. For panels 4b and 4d, the red contour line demarking thermocline is extremely difficult to see. In addition, the isotherms at depth (DO < 80 microM) are also difficult to see. For panels 4a and 4c, the 15_N line is difficult to spot as well.

These colors have been changed to white.

Figure 9. In panel 9a, white color in the IO domain has non-unique meaning. It can be either masked data or the transition from positive to negative correlation value. A way of uniquely distinguishing these should be used. Additionally, the white land mask is also not ideal but does have benefit of land-sea boundary.

We now use grey shade for the mask.

Panels 11a and 12 a-c. The combination of blue and black line colors is ineffective. Very difficult to distinguish between these two.

Black has been changed to red for better visual appeal.

Positive Indian Ocean Dipole events prevent anoxia off the west coast of India

V. Parvathi[1], I. Suresh[1], M. Lengaigne[2,3], C. Ethé[2], J. Vialard[2], M. Levy[2], S. Neetu[1], O. Aumont[2], L. Resplandy[4], H. Naik[1], S. W. A. Naqvi[1]

[1]CSIR-National Institute of Oceanography, Dona Paula, Goa 403 004, India
[2]LOCEAN-IPSL, Sorbonne Universités, LOCEAN (UPMC/CNRS/IRD/MNHN), Paris, France
[3]Indo-French Cell for Water Sciences, IISc-NIO-IITM–IRD Joint International Laboratory, NIO, Goa, India
[4]Scripps Institution of Oceanography, La Jolla, California, United States

Correspondence to: I. Suresh (isuresh@nio.org)

Abstract. The seasonal upwelling along the west coast of India (WCI) brings nutrient-rich, oxygen-poor subsurface waters to the continental shelf, favoring very low oxygen concentrations in the surface waters during late boreal summer and fall. This yearly-recurring coastal hypoxia is more severe during some years, leading to coastal anoxia that has strong impacts on the living resources. In the present study, we analyze a ¼°-resolution coupled physical-biogeochemical regional oceanic simulation over the 1960-2012 period to investigate the physical processes influencing the oxycline interannual variability off the WCI, that being a proxy for the variability on the shelf in our model. Our analysis indicates a tight relationship between the oxycline and thermocline variations in this region at both seasonal and interannual timescales, thereby revealing a strong physical control of the oxycline variability. As in observations, our model exhibits a shallow oxycline/thermocline during fall that combines with interannual variations to create a window of opportunity for coastal anoxic events. We further demonstrate that the boreal fall oxycline fluctuations off the WCI are strongly related to the Indian Ocean Dipole (IOD), with an asymmetric influence of its positive and negative phases. Positive IODs are associated with easterly wind anomalies near the southern tip of India. These winds force downwelling coastal Kelvin waves that propagate along the WCI and deepen the thermocline and oxycline there, thus preventing the occurrence of coastal anoxia. On the other hand, negative IODs are associated with WCI thermocline and oxycline anomalies of opposite sign, but of smaller amplitude, so that the negative or neutral IOD phases are necessary, but not the sufficient condition for coastal anoxia. As the IODs generally start developing in summer, these findings suggest some predictability to the occurrence of coastal anoxia off the WCI a couple of months ahead.

I. Suresh 26/12/2016 10:31 AM
Deleted: along

I. Suresh 26/12/2016 10:31 AM
Deleted: Matthieu…. Lengaigne[2,3], Christi ... [1]

I. Suresh 26/12/2016 10:31 AM
Deleted: leading to…avoring very low oxy ... [2]

1 Introduction

The continental shelf off the west coast of India (WCI) is home to the largest coastal hypoxic system of the world ocean, spreading over an area of ~180,000 km^2 (Naqvi et al., 2000). These hypoxic conditions, characterized by oxygen concentration lower than 20 μmol.l^{-1}, occur in fall, right after the southwest monsoon. Importantly, substantial year-to-year changes in both the duration and intensity of this seasonal oxygen deficiency have been reported in the literature (e.g. Naqvi et al., 2009). While the oxygen concentrations in near-bottom waters are systematically low enough to trigger conversion of oxidized nitrogen to molecular nitrogen, mostly through denitrification, this deficiency in some years is even more severe and the bottom waters turn sulphidic, a condition called coastal anoxia (Naqvi et al., 2006). These anoxic events have tremendous impact on living resources (e.g. Diaz and Rosenberg, 2008), with more frequent episodes of fish mortality and a shorter span of fishing season, inducing a sharp decline in fish catches.

Observations from a series of ship cruises during September – October 1999 (Naqvi et al., 2000) off the WCI and time-series measurements from a fixed site off Goa since 1997 (Naqvi et al., 2009) indicate the occurrence of severe hypoxic conditions over almost the entire shelf and anoxic conditions close to the WCI, with the most intense anoxic event reported in fall 2001 and moderate ones in fall 1998 and 1999. In contrast, these data indicate that fall 1997 was characterized by far less hypoxic conditions. The frequent anoxic conditions occurred during the 1998-2002 period were accompanied by a three to five-fold decline in demersal fish catch in 1999 and 2001 compared to 1997. The total fish landing also remained low between 1998 and 2002, adversely affecting the economy from fisheries, and the pelagic fish catches shifted from the dominance of mackerel to oil sardine from 1998 to 1999 (Krishnakumar and Bhat, 2008). There has been a remarkable revival of fisheries since 2003, apparently due to a relaxation of the intensity of oxygen deficiency, with no severe anoxic event reported over the recent years. Subsurface oxygen concentrations have also been reported to be significantly lower for the 1997–2004 period than for the 1971–1975 period (Naqvi et al., 2009). These observations thus reveal large interannual and decadal fluctuations in the oxygen deficiency along the WCI, but the processes responsible for these variations have not yet been understood (Naqvi et al., 2009).

As opposed to the other coastal hypoxic systems that have generally developed as a result of human activities (largely eutrophication) in the last few decades (Diaz and Rosenberg, 2008), the seasonal surface oxygen deficiency along the WCI is naturally driven. Indeed, it has been suggested that the oxygen-deficient conditions that develop in early fall along the WCI result from the seasonal upwelling, which brings poorly oxygenated sub-surface waters from the Oxygen Minimum Zone (OMZ) in the interior Arabian Sea (e.g. Morrison et al., 1999; Naqvi, 1987; Sarma, 2002) towards the surface along the continental shelf. This connection between the offshore and the shelf oxygen content has been discussed by several studies on the basis of in-situ oxygen observations along different cross-shelf transects. For example, Banse (1959) showed a clear

I. Suresh 26/12/2016 10:31 AM
Deleted: The

I. Suresh 26/12/2016 10:31 AM
Deleted: over the entire shelf off the WCI

I. Suresh 26/12/2016 10:31 AM
Deleted: in some years,

I. Suresh 26/12/2016 10:31 AM
Deleted: oxygen

I. Suresh 26/12/2016 10:31 AM
Deleted: severe

I. Suresh 26/12/2016 10:31 AM
Deleted: toward the surface (Fig. 1a). The thickest Oxygen Minimum Zone (OMZ) of the world's ocean is located in this region, between 100 and 1000-m depths (e.g. Morrison et al., 1999; Naqvi, 1987; Sarma, 2002). The coastal hypoxic conditions start with the onset of the seasonal upwelling that brings these OMZ waters to the shelf in August and cease with end of the upwelling season in December (Banse, 1959; Carruthers et al., 1959; Pillai et al., 2000).

association between the seasonal upwelling and coastal hypoxia on the shelf off Cochin at ~10°N in the last week of August 1957. A similar connection has also been reported by Carruthers et al. (1959) off Mumbai at 19°N in early November 1958 and later by Naqvi et al. (2009) off Mangalore at 13°N by late summer for several years. A recent study by Gupta et al. (2016) used ten shelf transects near 10^0 N during 2012 to conclude that the upwelling of oxygen-deficient waters along the shelf break during the monsoon is the major process regulating the biogeochemistry on the shelf. Although these studies indicate a clear connection between the shelf oxygen content and upwelling at the shelf break, the actual processes in these exchanges are not well understood, owing to the lack of continuous and high frequency observations.

The seasonal upwelling along the WCI starts in April but the shallowest thermocline marking the peak of the upwelling is usually observed during September-October (e.g. Schott and McCreary, 2001). Local alongshore winds are however only favorable to upwelling during the southwest monsoon (i.e., they only have an equatorward alongshore component from June to August). This is an indication that upwelling along the WCI is to a large extent forced by remote winds (Shetye et al., 1990). Wind variations in the equatorial band and Bay of Bengal indeed force coastal Kelvin waves that travel along the rim of the bay and up the WCI to influence the thermocline depth there (e.g. McCreary et al. 1993; Shetye, 1998). Recently, Suresh et al. (2016) demonstrated that wind variations in the vicinity of Sri Lanka are responsible for a large fraction of the seasonal upwelling along the WCI. On contrary to this seasonal variability of the upwelling and upper-ocean oxygen, there are currently little clues as to what causes the interannual variability along the WCI.

Identifying the main drivers of the near-surface oxygen interannual variations in regions of the main coastal hypoxic systems is an important endeavor as it may ultimately help to predict the occurrence of severe anoxic events. The large-scale climate modes have been suggested to influence the local oxygen variability in several coastal regions. For instance, the El Niño-Southern Oscillation (ENSO) strongly influences the oxygen concentrations along the coasts of Peru and Chile (Helly and Levine, 2004; Arntz et al., 2006; Gutierrez et al., 2008), with intensified oxygenation associated with weak El Niño upwelling and intensified hypoxia associated with strong La Niña upwelling. As in the Pacific, the natural climate variability in the Indian Ocean could also be a potential candidate responsible for the near-surface oxygen interannual variations along the WCI, but that has so far not been evaluated. The main indigenous mode of Indian Ocean interannual climate variability is the Indian Ocean Dipole (hereafter IOD; Saji et al., 1999; Webster et al., 1999; Murtugudde et al., 2000). A "positive" IOD is characterized by a cooling and anomalously shallow thermocline in the eastern Indian Ocean, and by a warming and anomalously deep thermocline in the central and western Indian Ocean, driven by anomalous easterlies in the central equatorial Indian Ocean. A "negative" IOD is associated with anomalous signals of opposite polarities. The IOD usually starts developing during boreal summer and peaks in fall (e.g. Saji et al., 1999). El Niño and La Niña events tend to induce respectively the positive and negative IODs in the Indian Ocean, but IOD can also occur independent of ENSO (e.g. Annamalai et al., 2003). The IODs induce larger-amplitude, large-scale wind and thermocline-depth variations than those

I. Suresh 26/12/2016 10:31 AM
Deleted: main thermocline …easonal upwe ... [3]

I. Suresh 26/12/2016 10:31 AM
Moved down [1]: Fig.

I. Suresh 26/12/2016 10:31 AM
Deleted: 1b) …re however only favorable t ... [4]

I. Suresh 26/12/2016 10:31 AM
Deleted: influence of …arge-scale climate ... [5]

associated with El Niño events over the Indian Ocean (e.g. Currie et al., 2013) and thus have the potential to affect the upwelling variations along the WCI through planetary wave propagation.

While the spatio-temporal density of observations in the eastern Pacific margin has allowed to accurately describe the monthly oxygen evolution along the west coast of South America over the past three decades (Helly and Levine, 2004; Arntz et al., 2006), there is a dearth of long-term data from fixed sites in the Indian Ocean as compared to the Pacific and the Atlantic (Gupta et al., 2016), which in turn prevents building a reliable time series that could depict the year-to-year variations. On the other hand, three-dimensional coupled physical-biogeochemical models that include the oxygen cycle have contributed to improve the description and understanding of dynamics of hypoxic events in various coastal regions (Pena et al., 2010), such as the Gulf of Mexico (e.g. Hetland and DiMarco, 2008), Black Sea (e.g. Gregoire and Friedrich, 2004) and Baltic Sea (e.g. Eilola et al., 2009). Such models have also been used to investigate the mechanisms driving the spatial distribution (McCreary et al., 2013) and seasonal evolution of the OMZ in the interior Arabian Sea (Resplandy et al., 2012). There is, however, no dedicated modeling study to date, addressing the mechanisms that drive the interannual oxygen variability along the WCI. The present study aims at identifying the physical controls of the WCI interannual oxygen variability, with the help of a 40-year long simulation from a ¼° regional coupled physical-biogeochemical model. While the ~25-km resolution of our model is insufficient to describe all the physical processes that influence the coastal upwelling (e.g. Huthnance 1995; Allen et al. 2010) or the shelf-open ocean interactions, we will show that our model still reproduces the essential characteristics of the large scale oxygen fluctuations off the shelf break, and that the offshore fluctuations provide a proxy for the variations on the shelf (Banse, 1959; Carruthers et al., 1959). Section 2 describes our model, data and methods, and provides a brief evaluation of the model. Section 3 describes the main seasonal features of the thermocline and oxycline variability along the WCI in both model and observations. The strong influence of the IOD on the interannual oxycline variations along the WCI is then assessed from the model analysis in section 4. Section 5 summarizes our results, discusses them in the context of earlier studies and assesses the limitations of our approach.

2 Data and methods

2.1 Observations

We used the 1°-resolution World Ocean Atlas-2013 (WOA13; Boyer et al., 2013) for evaluating the model accuracy at representing the large-scale climatological temperature and oxygen. The sea level is a good proxy for vertical movements of the thermocline in tropical regions (e.g. Fukumori et al., 1998), and hence we used the sea-level data from satellite altimetry produced by Ssalto/Duacs and distributed by AVISO (http://www.aviso.altimetry.fr/duacs/) as a proxy for the thermocline interannual variability along the WCI. In addition, we used the monthly level 3 Ocean Color Climate Change Initiative (OC-CCI) product, available at http://www.oceancolour.org/, that merges data from the SeaWiFs, MERIS and MODIS ocean color missions to evaluate the model surface chlorophyll climatological seasonal cycle.

I. Suresh 26/12/2016 10:31 AM
Deleted: dynamics

I. Suresh 26/12/2016 10:31 AM
Deleted: describe

I. Suresh 26/12/2016 10:31 AM
Deleted: major

I. Suresh 26/12/2016 10:31 AM
Deleted: of the

I. Suresh 26/12/2016 10:31 AM
Deleted: modelling

I. Suresh 26/12/2016 10:31 AM
Deleted: The horizontal

I. Suresh 26/12/2016 10:31 AM
Deleted: too coarse

I. Suresh 26/12/2016 10:31 AM
Deleted: resolve the dynamics on the continental shelf, but should allow identifying

I. Suresh 26/12/2016 10:31 AM
Deleted: -

I. Suresh 26/12/2016 10:31 AM
Deleted: processes controlling

I. Suresh 26/12/2016 10:31 AM
Deleted: oxygen variability, which in turn control

I. Suresh 26/12/2016 10:31 AM
Deleted: supply of oxygen to

I. Suresh 26/12/2016 10:31 AM
Deleted: Gupta

I. Suresh 26/12/2016 10:31 AM
Deleted: 2016

I. Suresh 26/12/2016 10:31 AM
Deleted: the

I. Suresh 26/12/2016 10:31 AM
Deleted: ,

I. Suresh 26/12/2016 10:31 AM
Deleted: the

I. Suresh 26/12/2016 10:31 AM
Deleted: model

I. Suresh 26/12/2016 10:31 AM
Deleted: and

I. Suresh 26/12/2016 10:31 AM
Deleted: against previous

I. Suresh 26/12/2016 10:31 AM
Deleted: being

We also used oxygen measurements from Candolim Time Series (CaTS) station located on the WCI in the inner shelf off Goa (~15.5°N; 73.6°E) to construct a seasonal cycle of oxygen variations near the coast. This station has been established by Council of Scientific and Industrial Research-National Institute of Oceanography (CSIR-NIO) and records the physical (temperature, salinity) and biogeochemical (oxygen, nitrate, nitrite, hydrogen sulphide, etc.) parameters from September 1997 onwards (see Maya et al., 2011 for a detailed description). This site lies approximately 10 km off the Candolim beach, where the depth of the water column is ~28m. Samples are taken at four depths: just below the surface, just above the bottom, and at two intermediate depths equally spaced between the surface and bottom. This dataset consists of a total of 142 vertical profiles during the 1997-2010 period and has been extensively used by the previous studies (e.g., Naqvi et al., 2006, 2009, 2010a). Fig. 1a shows the percentage of years sampled month-wise in this dataset. It indicates that in-situ measurements have been performed at this station ~50% of the years over the 1997-2010 period for most calendar months, including September-October (the time of peaking of anoxic events), except for June (< 10%) and July (no data), when summer monsoon rough weather conditions prevent observations (Naqvi et al., 2009). This temporal coverage allows us to build a reliable monthly climatology of near-coastal oxygen variations, except for the month of June and July. Though CaTS offers the best available dataset to study the oxygen variations along the WCI, a thorough description of oxygen interannual variability is limited by two reasons. First, during our period of interest, i.e., September – October, the temporal distribution of the data indicates that only ~50% of the years were sampled over the 1997-2010 period. Second, the months for which a large number of records are available reveal very different vertical oxygen profile over the same month (like in September 1998 or 2000; Figs. 1c and 1e), highlighting the existence of a large variability at sub-monthly timescale. For some other months, the number of available profiles is very limited, like in September 1999, when only one profile is available (Fig. 1d). Given the existing high frequency variability, averaging this very limited number of profiles may not provide a value representative of the actual monthly average. As a result, the uneven temporal distribution and the sub-monthly variability do not allow us to build a reliable monthly pluri-annual time series from this dataset. In addition, these observations collected at a single coastal site may be influenced by local processes and hence may not be representative of the dynamics along the entire WCI. We will hence identify the years when severe oxygen deficiency occurs from Table 1 of Naqvi et al. (2009), which is based on the absence of nitrate and nitrite and the presence of hydrogen sulphide in the water column. These years will be further discussed and compared with our model results at the end of this paper.

I. Suresh 26/12/2016 10:31 AM
Deleted: the

I. Suresh 26/12/2016 10:31 AM
Deleted: along

I. Suresh 26/12/2016 10:31 AM
Deleted: CSIR

I. Suresh 26/12/2016 10:31 AM
Deleted: 2a

I. Suresh 26/12/2016 10:31 AM
Deleted: 2cand 2e

I. Suresh 26/12/2016 10:31 AM
Deleted: 2d

I. Suresh 26/12/2016 10:31 AM
Deleted: ,

I. Suresh 26/12/2016 10:31 AM
Deleted: are marked as black stars on

I. Suresh 26/12/2016 10:31 AM
Moved down [2]: Fig.

I. Suresh 26/12/2016 10:31 AM
Deleted: 11b and

2.2 Model description

The model used in this study couples the NEMO (Nucleus for European Modelling of the Ocean; Madec, 2008) physical ocean component with the PISCES (Pelagic Interaction Scheme for Carbon and Ecosystem Studies; Aumont et al., 2015) biogeochemical component through the OASIS3 (Valcke, 2013) coupler. The PISCES model has 24 compartments, which include two sizes of sinking particles and four "living" biological pools, representing two phytoplankton (nano-phytoplankton and diatoms) and two zooplankton (microzooplankton and meso-zooplankton) size classes. Phytoplankton

growth is limited by five nutrients: NO3, NH4, PO4, SiO4, and Fe. The ratios among C, N, and P are kept constant for the "living" compartments, at values proposed by Takahashi et al. (1985). The internal Fe contents of both phytoplankton groups and Si contents of diatoms are prognostically simulated as a function of ambient concentrations in nutrients and light level. Details on the red-green-blue model from which light penetration profiles are calculated are given in Lengaigne et al. (2007). The Chl/C ratio is modeled using a modified version of the photo-adaptation model by Geider et al. (1998). Dissolved oxygen is prognostic and evolves in response to physical conditions (advection, mixing), biological sources and sinks and the air-sea fluxes:

$$\partial_t O_2 = \underbrace{\left(\frac{\partial O_2}{\partial t}\right)_{Dyn}}_{Dynamical\ Transport} + \underbrace{\left(\frac{\partial O_2}{\partial t}\right)_{Bio}}_{Biological\ sources\ \&\ sinks} + J_{flux}$$

where $(\partial O_2/\partial t)_{Bio}$ includes all biological processes affecting the concentration of O_2, $(\partial O_2/\partial t)_{Dyn}$ accounts for large scale and turbulent transport of oxygen and J_{flux} is the contribution of O_2 air–sea fluxes. The response of oxygen to biological processes $(\partial O_2/\partial t)_{Bio}$ is computed as follows:

$$\left(\frac{\partial O_2}{\partial t}\right)_{Bio} = \underbrace{(R^1_{o:c} + R^2_{o:c})\left(\mu^P_{NO_3}P + \mu^D_{NO_3}D\right)}_{New\ Production} + \underbrace{R^1_{o:c}\left(\mu^P_{NH_4}P + \mu^D_{NH_4}D\right)}_{Regenerated\ Production} - \underbrace{\lambda^*_{DOC} f(O_2) DOC}_{Reminralization} - \underbrace{G^Z Z - G^M M}_{Respiration} - \underbrace{R^2_{o:c} Nitrif}_{Nitrification}$$

Oxygen is produced during photosynthesis (calculating the uptake of nitrate and ammonium by phytoplankton separately) by nanophytoplankton (P) and diatoms (D) and consumed by dissolved organic matter (DOC) remineralization, small (Z) and large (M) zooplankton respiration, and nitrification. This last term represents the conversion of ammonium into nitrate and is assumed to be photo-inhibited, and reduced in suboxic waters. It is therefore a function of the ammonium and oxygen concentrations and photosynthetically available radiation. In this equation, the stoichiometric ratio $R^1_{o:c}$ represents the change in oxygen relative to carbon during ammonium conversion into organic matter, whereas $R^2_{o:c}$ denotes the consumption of oxygen during nitrification. Their values have been set respectively to 131:122 and 32:122 so that the typical Redfield ratio for oxygen is equal to 1.34 as proposed by Kortzinger et al. (2001).

When oxygen falls below a threshold value set to 6 µmol.L^{-1}, nitrate instead of oxygen starts to be increasingly consumed during the remineralization of organic matter, i.e., denitrification. To avoid negative oxygen concentration in the model, all processes consuming oxygen are switched off below a 10^{-3} µmol.L^{-1} threshold. Anammox is not represented in the

I. Suresh 26/12/2016 10:31 AM
Deleted: modelled

I. Suresh 26/12/2016 10:31 AM
Deleted: $\underbrace{\left(\frac{\partial O_2}{\partial t}\right)_{Dyn}}_{Dynamical\ transport} + \underbrace{\left(\frac{\partial O_2}{\partial t}\right)_{Bio}}_{Biological\ sources\ and\ sinks} + J_{flux}$

model. At the bottom of the ocean, the model includes a very simple description of the sediment processes. The metamodel of Middelburg et al. (1996) is further used to compute the relative contribution of denitrification to the remineralization of the organic matter. Then, the flux of organic matter to the sediment is used to compute the oxygen and nitrate demands in the sediment, which are then imposed as boundary conditions to the model.

The response of oxygen to dynamical processes is computed as:

$$\left(\frac{\partial O_2}{\partial t}\right)_{Dyn} = \underbrace{-u_H \cdot \nabla_H O_2}_{lateral\ advection} - \underbrace{w \cdot \nabla_H O_2}_{vertical\ advection} + \underbrace{\frac{\partial K_z \partial O_2}{\partial z^2}}_{vertical\ mixing}$$

where u_H and w are respectively the horizontal and vertical currents and K_z is the vertical mixing coefficient computed by the dynamical model.

Finally, J_{flux} is the air-sea flux of O_2 (F_{O_2}) divided by the depth of model surface layer, where

$$F_{O_2} = k_w(\alpha O_{2atm} - O_2)$$

k_w is the transfer velocity, $(\alpha O_{2atm} - O_2)$ is the difference in O_2 partial pressure between the air and surface sea water, and α the solubility of O_2 in seawater.

The NEMO-PISCES coupled biophysical model has been successfully applied to various studies in the Indian Ocean (e.g. Kone et al., 2009; Resplandy et al. 2009; Currie et al., 2013; Keerthi et al. 2016), including the Arabian Sea OMZ (Resplandy et al., 2011, 2012). A more detailed model description is provided in the manuals for NEMO and PISCES available online at http://www.nemo-ocean.eu/About-NEMO/Reference-manuals.

Here, we specifically use a ¼° resolution (i.e. cell size ~25 km) Indian Ocean regional configuration, which is a sub-domain of the global configuration described by Barnier et al. (2006). It has 46 vertical levels, with a resolution ranging from 5m at the surface to 250m at the bottom. The African continent closes the western boundary of the domain. The oceanic portions of the eastern, northern and southern boundaries use radiative open boundaries (Treguier et al., 2001), constrained with a 150-day timescale relaxation to physical and biogeochemical inputs from a global simulation (Dussin et al., 2009). The circulation and thermodynamics of this regional configuration have been extensively evaluated and found to perform well in several Indian Ocean regions (Praveen Kumar et al., 2014), including the Arabian Sea (Nisha et al., 2013; Vialard et al., 2013; Keerthi et al., 2015, 2016) and the Bay of Bengal (Akhil et al., 2014, 2016).

I. Suresh 26/12/2016 10:31 AM
Deleted: .

I. Suresh 26/12/2016 10:31 AM
Deleted: from air to sea

I. Suresh 26/12/2016 10:31 AM
Deleted: For a more detailed description, manuals for NEMO and PISCES are available online at http://www.nemo-ocean.eu/About-NEMO/Reference-manuals. This coupled

I. Suresh 26/12/2016 10:31 AM
Deleted: The

I. Suresh 26/12/2016 10:31 AM
Deleted: used in the following

I. Suresh 26/12/2016 10:31 AM
Deleted: an Indian Ocean

I. Suresh 26/12/2016 10:31 AM
Deleted: from

I. Suresh 26/12/2016 10:31 AM
Deleted: ¼° resolution (i.e. cell size ~25 km)

I. Suresh 26/12/2016 10:31 AM
Deleted: shown to reproduce observed intraseasonal variations of key physical parameters

The simulation starts from the rest and the WOA13 climatology temperature and salinity (Boyer et al., 2013). PISCES biogeochemical tracers are initialized from the WOA13 database for nutrients and a global simulation climatology for other tracers (Aumont and Bopp, 2006). After 5 years of spin-up with climatological surface and lateral boundary forcing, the model is forced with the Drakkar Forcing Set #4.4 (DFS4.4, Brodeau et al., 2009) from 1958 to 2012. This forcing is a modified version of the CORE dataset (Large and Yeager, 2004), with atmospheric parameters derived from ERA40 reanalysis until 2002 (Uppala et al., 2005) and ECMWF analysis after 2002 for latent and sensible heat fluxes computation. Radiative fluxes are taken from the corrected International Satellite Cloud Climatology Project-Flux Dataset (ISCCP-FD) surface radiations (Zhang et al., 2004), while precipitation are specified from a blend of satellite products described in Large and Yeager (2004). All atmospheric fields are corrected to avoid temporal discontinuities and to remove known biases (see Brodeau et al., 2009 for details). In the following, the 1960-2012 period is analyzed.

I. Suresh 26/12/2016 10:31 AM
Deleted: are initialized from the WOA13 climatology…(Boyer et al., 2013). PISCES ... [6]

2.3 Model climatology

The model's ability to capture the climatological surface chlorophyll concentrations during the summer and winter monsoons is illustrated on Fig. 2. During summer monsoon (Fig. 2a), seasonal blooms are observed along the coasts of the Arabian Peninsula and along the WCI in response to coastal upwelling that brings nutrients into the euphotic layer (e.g. Wiggert et al., 2005; Levy et al., 2007; Koné et al., 2009). The chlorophyll signal along the Somalia and Omani coasts extends offshore towards the central Arabian Sea (Fig. 2a) through offshore lateral advection of nutrients from upwelling regions, either by large-scale circulation or by eddy activity (e.g. Lee et al., 2000; Resplandy et al., 2011). During winter monsoon (Fig. 2b), the cool, dry northeasterly winds in the Arabian Sea induce convective mixing and entrain nutrient-rich waters to the surface, triggering the chlorophyll bloom observed north of 15°N (Madhupratap et al., 1996). The model generally accurately reproduces these seasonal chlorophyll patterns (Figs. 2c and 2d). As for observations, the largest chlorophyll bloom in summer occurs in the western Arabian Sea, with strong signals along the rim of the northern Indian Ocean, while winter is characterized by oligotrophic conditions in the southeastern Arabian Sea and higher concentrations in the northern and western parts. The largest discrepancy between modeled and satellite chlorophyll is an overall overestimation of the amplitude of the summer blooms, in the western Arabian Sea, east of Sri Lanka and around the rim the Bay of Bengal (Figs. 2a and 2c). The seasonal chlorophyll patterns in fall are very similar, although weaker than those in summer in both observations and model (not shown).

I. Suresh 26/12/2016 10:31 AM
Deleted: shown in…llustrated on Fig. 3…. ... [7]

The comparison of the modeled horizontal and vertical climatological oxygen distribution with that of WOA13 is shown in Fig. 3. In observations, the core of the OMZ is confined to the northern part of the basin (Fig. 3a) and expands vertically between 150 and 1000-m depth (Fig. 3b), with lowest subsurface oxygen concentrations found in the central/eastern part of the basin. The OMZ is thus shifted to the east of the region of highest biological production located along the west coast of the Arabian Sea (Fig. 2). The oxycline lies around ~100m, and is slightly shallower on the western and eastern part of the basin (Fig. 3b), because of the seasonal upwelling systems there. The model captures these observed oxygen patterns, with

I. Suresh 26/12/2016 10:31 AM
Deleted: modelled…odeled horizontal and ... [8]

poorly-oxygenated water confined to the northern Arabian Sea and high-oxygenated water found near the equator and farther south, and an OMZ core located in the eastern part of the Arabian Sea despite a slight overestimation of the modeled oxygen content at depth in the Arabian Sea (Figs. 3b vs 3d). We can also note that the model underestimates the depth of the OMZ core (~200m in the model and ~300m in observations). The upper ocean vertical oxygen distribution is well captured, with a model oxycline depth around 100m (Fig. 3d), similar to the observed one (Fig. 3c).

2.4 Thermocline and oxycline depths

Both temperature and dissolved oxygen decrease with increasing depth below the mixed layer (Figs. 3b and d). The oxycline or thermocline depths are defined as the depths of maximum gradient. It is however customary to approximate those depths from a fixed isocontour, especially in tropical regions. Resplandy et al. (2012) used the depth of 100 µmol L^{-1} as a proxy for the oxycline depth in their study, whereas Prakash et al. (2013) used 50 µmol L^{-1}. Here, we define the oxycline depth (hereafter OCD) as the depth of the 100 µmol L^{-1} oxygen isocontour (following Resplandy et al., 2012) and the thermocline depth (hereafter TCD) as the depth of 23^{o} C isotherm (following Prakash et al., 2013). The conclusions of our study are not sensitive to the above choices in the northern Indian Ocean (and especially in our focus region along the WCI), i.e., the results discussed below are similar when considering the 50 µmol L^{-1} or 150 µmol L^{-1} instead of 100 µmol L^{-1}, to define the oxycline depth and 20°C or 25°C instead of 23°C to define the thermocline depth. The OCD and TCD were both derived from observed or modeled profiles using linear interpolation. To ascertain the variability along the WCI, we average relevant parameters over a box located between 10°N and 15°N extending from the coast to 2° offshore (hereafter referred to as the WCI box, shown on Fig. 5). It must be noticed that the results discussed below are not sensitive to any slight modifications of the box boundaries or offshore extent of this box. Interannual anomalies of all variables are calculated from monthly time-series by subtracting the mean seasonal cycle and applying a 3-month smoothing to remove the sub-seasonal variations.

2.5 IOD index

To characterize the IOD variability, we used the standard definition of the Dipole Mode Index (DMI, Saji et al., 1999), which is calculated as the difference between the interannual SST anomalies in the western (50°E-70°E; 10°N-10°S) and southeastern (90°E-110°E; 10°S-0°) equatorial Indian Ocean averaged over September–November. We have used the DMI derived from observed SST, but the very high correlation between the DMI based on model and observations (~0.94) make our results fairly insensitive to the choice of either model or observationally-based DMI. This index has been normalized by its standard deviation to make it dimensionless.

I. Suresh 26/12/2016 10:31 AM
Deleted: modelled

I. Suresh 26/12/2016 10:31 AM
Deleted: Fig. 4b

I. Suresh 26/12/2016 10:31 AM
Deleted: Fig. 4d

I. Suresh 26/12/2016 10:31 AM
Deleted: also

I. Suresh 26/12/2016 10:31 AM
Deleted: 4d

I. Suresh 26/12/2016 10:31 AM
Deleted: 4c).

I. Suresh 26/12/2016 10:31 AM
Deleted: 4b

I. Suresh 26/12/2016 10:31 AM
Deleted: usually

I. Suresh 26/12/2016 10:31 AM
Deleted: l

I. Suresh 26/12/2016 10:31 AM
Deleted: l

I. Suresh 26/12/2016 10:31 AM
Deleted: l

I. Suresh 26/12/2016 10:31 AM
Deleted: ,

I. Suresh 26/12/2016 10:31 AM
Deleted: l

I. Suresh 26/12/2016 10:31 AM
Deleted: l

I. Suresh 26/12/2016 10:31 AM
Deleted: l

I. Suresh 26/12/2016 10:31 AM
Deleted: modelled profiles using linear interpolation.

I. Suresh 26/12/2016 10:31 AM
Deleted: in

I. Suresh 26/12/2016 10:31 AM
Deleted: For consistency, we

I. Suresh 26/12/2016 10:31 AM
Deleted: the model

I. Suresh 26/12/2016 10:31 AM
Deleted: 87

I. Suresh 26/12/2016 10:31 AM
Deleted: of them.

I. Suresh 26/12/2016 10:31 AM
Deleted: . Interannual anomalies are calculated from monthly time-series by subtracting the ... [9]

3 Results

3.1 Dynamical control of the oxycline variability along the WCI

The seasonality of the oxygen concentration within the core of the OMZ is very weak, but this is not the case for the OCD (Resplandy et al., 2012). Fig. 4 shows the depth-time section of the oxygen and temperature seasonal cycle off the WCI (see black frame on Fig. 5 for the WCI box location) from both model and observations. This figure illustrates that the seasonal evolution of temperature and oxygen are very similar, with both OCD and TCD start shoaling in April (~ 100 m) and reaching their shallowest depth during September-October (~50 m). This figure thus indicates a tight coupling between the oxycline and thermocline depth variations off the WCI. Resplandy et al. (2012) performed a budget analysis of the terms contributing to the seasonal oxygen variability along the WCI, and showed that, although the biological sink and the dynamical sources of oxygen compensate on annual average, the oxygen seasonality in this region primarily arises from the vertical advection of oxygen. Vertical velocities act in the same way on the oxygen and temperature isolines, lifting or lowering them in phase as illustrated in Fig. 4, resulting in strong correlation between OCD and TCD along the WCI.

The above close link between the thermocline and oxycline has also been observed in many regions (e.g., Morales et al., 1999; Prakash et al., 2013). Fig. 5 quantifies this relationship for the entire northern Indian Ocean by displaying the correlation between the seasonal OCD and TCD variations for both observations and model, and these correlations exceed 0.7 everywhere in the Arabian Sea, except in a small region off the Horn of Africa. These correlations drop in the equatorial region, presumably because our oxycline definition (100 µmol L^{-1}) corresponds to a lower temperature criterion than 23°C (for defining TCD) in that region. The model in general exhibits higher OCD-TCD correlations than in the observations, especially in the eastern Bay of Bengal where observed OCD and TCD are not well correlated. The tight OCD-TCD relationship along the WCI implies a strong control of seasonal oxygen variability by the upwelling intensity in that region.

This tight relation between the OCD and TCD is further illustrated in Fig. 6, which displays spatial maps of observed and modeled OCD and TCD seasonal climatologies. During the spring inter monsoon (March-May), the TCD and OCD are spatially quite uniform and deep (~100 m) in the southeastern Arabian Sea (Figs. 6a and 6e). This is also the case along the WCI south of 15°N despite the local upwelling favorable alongshore winds, indicating a remote control of OCD and TCD variations there. In contrast, the shallower OCD/TCD near the Southern Tip of India (STI) during this season is consistent with upwelling favorable winds in this region (Figs. 6a and 6e). With the advent of the summer monsoon (June-August), the westerly monsoon winds drive a very strong offshore Ekman transport in the western Bay of Bengal and near the STI (Suresh et al., 2016), resulting in an upwelling signal, which shoals the OCD/TCD up to 60 m at the STI (Figs. 6b and 6f; Smitha et al., 2008; Gupta et al., 2016). Further north, the winds are almost perpendicular to the coast of western India (Suresh et al., 2016) and hence do not induce upwelling there. The shallow OCD/TCD signal from the STI propagates northward along the western Indian coast as an upwelling coastal Kelvin wave (Suresh et al., 2016; see Figs. 6b and 6f), with

I. Suresh 26/12/2016 10:31 AM
Deleted: 1a suggests… shows the depth-ti ... [10]

I. Suresh 26/12/2016 10:31 AM
Moved down [3]: been observed in many regions (e.g., Morales et al., 1999; Prakash et al., 2013).

I. Suresh 26/12/2016 10:31 AM
Deleted: This is expected in regions, where the effects of …iological processes and of verti ... [11]

I. Suresh 26/12/2016 10:31 AM
Moved (insertion) [3] ... [12]

I. Suresh 26/12/2016 10:31 AM
Deleted: . Figs. 5a and 5b quantify… quar ... [13]

I. Suresh 26/12/2016 10:31 AM
Deleted: The…his tight relation between t ... [14]

OCD/TCD patterns clearly suggestive of faster wave propagation at lower latitudes. By the end of the southwest monsoon (September-October-November, hereafter SON), shallow OCD/TCD can be seen along the entire Arabian Sea coastal rim, primarily resulting from the remotely-forced coastal Kelvin waves. From December to February, winds at the STI and alongshore winds further north are both favorable to downwelling, thus leading to deepening of the TCD and OCD along the WCI (Figs. 6d and 6h). Part of the strong upwelling signal at the coast during the preceding season (Figs. 6c and 6g) is radiated westward as a planetary wave (Figs. 6d and 6h; e.g. McCreary et al., 1993, Suresh et al., 2016). The striking similarity in the seasonal patterns of OCD and TCD again indicates a strong physical control of the eastern Arabian Sea OCD at the seasonal timescale. This echoes results of Resplandy et al. (2012), who found that upper-ocean oxygen seasonality primarily arises from vertical movements at the thermocline level forced by both local and remote wind forcing.

In order to further illustrate the remote forcing effects discussed above, and the connection between the offshore oxygen variability and that on the shelf, Fig. 7 shows the seasonal evolution of remote and local winds (Fig. 7a) and a comparison of the climatological near-surface oxygen contents (0-40m average) obtained from the model and WOA13 offshore to the WCI (i.e. in the WCI box) with those obtained from the CaTS on the shelf (Figs. 7b and c). The modeled and WOA oxygen climatologies in the WCI box match very well for the entire year. In contrast, the CaTs in-situ measurements show lower oxygen concentrations. The oxygen concentration on the shelf is expected to be lower than that offshore because of a higher oxygen consumption on the shelf, particularly associated with sediment respiration process, which in our model is a very simple representation. Despite lower oxygen content on the shelf, there is a very good phase agreement between the oxygen seasonal variations from CaTS in-situ measurements and the corresponding offshore variations derived from the WOA and model, suggesting a strong offshore-shelf connection through dynamical upwelling process, as suggested by Banse (1959), Carruthers et al. (1959) and Gupta et al. (2016).

The seasonal wind evolution shown in Fig. 7a allows discussing the respective influences of local (WCI box) and remote forcing (at STI) in driving the seasonal oxycline variations along the WCI. As discussed above (e.g. Fig. 4), the upwelling off WCI starts developing (reduction in upper ocean oxygen content) at the beginning of the summer monsoon (April-May), reaches a maximum (minimum upper ocean oxygen content) by September-October and decays (increase upper ocean oxygen content) by November. The local winds along the WCI (black continuous curve on Fig. 7a) are favorable to upwelling only during the southwest monsoon (i.e., they have an alongshore southward component only from June to August), which indicates that the upwelling along the WCI is to a large extent driven by remote winds (Shetye et al., 1990). The wind near the STI is upwelling-favorable from about April to October, and hence matches the seasonality of the upwelling of cold and low-oxygen waters, in agreement with the results of Suresh et al. (2016).

The gaps in the CaTS observational dataset do not allow constructing a reliable time series of interannual upper ocean oxygen content, to which our model could be validated. However, the data can still provide some estimate of the amplitude

I. Suresh 26/12/2016 10:31 AM
Deleted: largely as the result of

I. Suresh 26/12/2016 10:31 AM
Deleted: (Figs. 6d, 6h and 1b),

I. Suresh 26/12/2016 10:31 AM
Deleted: downwelling

I. Suresh 26/12/2016 10:31 AM
Deleted: This is clearly shown in the model, where the shape of the deep OCD/TCD pattern is clearly suggestive of faster planetary wave propagation at lower latitudes (Fig. 6h).

I. Suresh 26/12/2016 10:31 AM
Deleted: The observed

I. Suresh 26/12/2016 10:31 AM
Deleted: modelled seasonal oxycline

I. Suresh 26/12/2016 10:31 AM
Deleted: along the WCI (box shown in Figs. 1c and 5) are further illustrated

I. Suresh 26/12/2016 10:31 AM
Deleted: Fig. 7. The modelled and observed climatologies

I. Suresh 26/12/2016 10:31 AM
Moved (insertion) [2]

I. Suresh 26/12/2016 10:31 AM
Deleted: , a pre-requisite for using the model for understanding the processes of interannual oxycline variability there. Consistent with previous figures, the oxycline

I. Suresh 26/12/2016 10:31 AM
Deleted: shoaling

I. Suresh 26/12/2016 10:31 AM
Deleted: becomes shallowest

I. Suresh 26/12/2016 10:31 AM
Deleted: then starts deepening again by November. In addition to this seasonal evolution, Fig. 7 also provides an estimation

of interannual variability, which can be compared to that of our model (the whiskers on Figs. 7b and 7c indicate the amplitude of the variability around the mean seasonal cycle). Despite a slight underestimation in our model, the amplitude of the near-surface oxygen interannual variability is largest during SON, both in the shelf observations and the model. This further corroborates the offshore-shelf connection discussed above.

A seasonally shallow OCD combined with a larger interannual variability in fall creates a window of opportunity for the occurrence of coastal anoxic events. Figs. 7d and 7e display the monthly percentages of occurrence of hypoxic profiles from CaTS (on the shelf) data and the model (offshore). While the general patterns of oxygen/oxycline variability on the shelf and offshore to the coast remain similar, the actual upper ocean oxygen content and vertical oxygen profiles are different. Hence, we have used different thresholds to detect hypoxic profiles in the observation and the model. Consistent with previous literature, anoxic events are most likely to occur from August to November in the model and the shelf data, as expected from the very shallow background oxycline at that time of the year. This justifies our focus on the fall period for analyzing the processes that drive the modeled interannual variability of the WCI oxycline in the following.

We previously demonstrated a tight relationship between the seasonal variability of OCD and TCD in the eastern Arabian Sea. Fig. 8a exhibits a similar relation in large portions of the northern Indian Ocean for fall interannual OCD and TCD anomalies in the model. A comparison with observations is unfortunately not feasible due to lack of a basin-scale dataset for interannual OCD anomalies. The correlation between interannual OCD and TCD anomalies are, in general, slightly weaker than that at seasonal timescales (Fig. 5b), but remain high in a large part of the Indian Ocean north of 5°N, generally exceeding 0.8 in the entire Bay of Bengal and in the eastern Arabian Sea, and in particular in the WCI box (~0.95 correlation, Fig. 8b).

The influence of remote forcing at WCI is further established in Fig. 9. Due to unavailability of the continuous oxygen observations (see Section 2.1), we cannot directly evaluate the modeled oxygen interannual variability in the WCI region. We however evaluate the modeled TCD interannual variability, which is closely tied to the OCD interannual variability (~0.95 correlation, Fig. 8b). The modeled interannual TCD anomalies in the WCI box (red curve on Fig. 9a) agree well (0.84 correlation) with sea-level interannual anomalies (a good proxy for TCD variations in stratified regions) from altimeter measurements (blue curve on Fig. 9a) during fall. Despite instances, when the model agreement is weaker, like during 2002-2006 period, both the modeled TCD and the observed sea level indicate strongest thermocline shoaling in fall 1999 and deeper than usual thermocline in fall 1994, 1997 and 2008. We will exploit this ability of our model to capture the observed TCD interannual variations along the WCI to further examine the processes responsible for the OCD interannual variability. Along with fall TCD and sea-level anomalies at WCI, Fig. 9a also displays the fall interannual anomalies of zonal winds at the STI (black dashed curve on Fig. 9a; box with dashed frame in Figs. 9b and 9c). The good phase agreement between the interannual fluctuations of zonal winds at STI and both modeled TCD and observed SLA (-0.65 and -0.69 correlation

I. Suresh 26/12/2016 10:31 AM
Deleted: the …nterannual OCD …ariabili ... [15]

I. Suresh 26/12/2016 10:31 AM
Deleted: coastal anoxic events to occur during September-November (hereafter SON). This is consistent with previous observations of oxygen deficiency along the WCI (e.g., Naqvi et al., 2000, 2009; Gupta et al., 2016). ... [16]

I. Suresh 26/12/2016 10:31 AM
Deleted: connection…elationship betwee ... [17]

I. Suresh 26/12/2016 10:31 AM
Deleted: the …navailability of the continu ... [18]

respectively, Fig. 9a) at WCI is a strong indication that the interannual variations along the WCI are strongly influenced by the wind variations at the STI, through coastal Kelvin waves propagation, as demonstrated by Suresh et al. (2016) for the seasonal timescale. Fig. 9b shows the correlation of interannual anomalies of model TCD everywhere in the northern Indian Ocean with the time series of model TCD in the WCI box during fall. Fig. 9c shows a similar analysis, but for the observed SLA. In both model and observations, the thermocline depth variations along the WCI in fall are associated with basin-scale coherent signals in thermocline depth, sea level and wind stresses. Those basin-scale patterns are very similar to those associated with a positive phase of the IOD mode, with upwelling in the Eastern Equatorial Indian Ocean (EEIO) and a downwelling in the western Indian Ocean. In the following section, we will show how IOD events influence the fall thermocline and oxycline depths off the WCI.

The relationships between the modeled interannual variability of the OCD along the WCI and that of the OCD, TCD, SST and wind at the basin scale are demonstrated in Figs. 10a and 10b, which show regression maps of fall interannual anomalies of these variables to the time series of the fall WCI OCD anomalies shown in Fig. 8b (black line) over the 1960-2012 period. These maps display the typical basin-scale anomalies corresponding to an anomalously deep OCD in the WCI. Consistent with Fig. 9, the fall WCI OCD variations are not merely local, but are associated with basin-scale ocean-atmosphere interannual anomalies over the entire equatorial and northern Indian Ocean. An anomalously deep OCD off the WCI is usually associated with deeper OCD and TCD (i.e. positive anomalies) in the southeastern Arabian Sea and in the vicinity of Sri Lanka and the STI (Figs. 10a and 10b). Positive OCD anomalies off the WCI are also related to shallower OCD and TCD in the eastern Indian Ocean and along the eastern rim of the Bay of Bengal (i.e. negative anomalies). The associated large-scale wind patterns (Fig. 10a) explain these interannual OCD and TCD patterns. Anomalous easterlies in the equatorial band force upwelling equatorial Kelvin waves that shoal the OCD and TCD in the EEIO. These signals further propagate around the rim of the Bay as upwelling coastal Kelvin waves, thereby shoaling the TCD and OCD there (e.g. McCreary et al., 1993; McCreary et al. 1996; Aparna et al., 2012). Similar to what happens at the seasonal scale (Suresh et al., 2016), easterly zonal wind stress anomalies in the vicinity of Sri Lanka and the STI force a downwelling coastal Kelvin wave that propagates poleward along the western Indian coastline, resulting in deepening of the TCD and OCD there. The strong negative correlation between the WCI OCD and STI zonal winds interannual fluctuations (-0.73 over the entire period; see Fig. 11b) further illustrates the strong influence of these winds in driving OCD and TCD interannual fluctuations in the southeastern part of the Arabian Sea. In contrast, the local alongshore wind variations along the WCI have a weaker influence on the WCI OCD, with a negative correlation of -0.25 (Fig. 11c), confirming the dominance of remote forcing from the STI region over the influence of local winds.

The SST variations associated with the OCD signals in the WCI region are characterized by a clear signal in the EEIO (near the Sumatra coast), and weaker signals of opposite sign in the western Indian Ocean. As pointed out before, the patterns shown on Figs. 9b, 9c and Fig. 10a, 10b are reminiscent of the IOD signature (Saji et al., 1999; Webster et al. 1999;

I. Suresh 26/12/2016 10:31 AM
Moved (insertion) [4]

I. Suresh 26/12/2016 10:31 AM
Deleted: there

I. Suresh 26/12/2016 10:31 AM
Deleted: 3.2 The IOD control on the oxycline interannual variability along the WCI ... [19]

I. Suresh 26/12/2016 10:31 AM
Moved up [4]: Fig.

I. Suresh 26/12/2016 10:31 AM
Deleted: 10b, these variations are also related to anomalous SST patterns characterized by a strong cooling south of the equator in the eastern Indian Ocean and a weaker warming in the western portion of the basin.

I. Suresh 26/12/2016 10:31 AM
Deleted: TCD, …ST variations associated ... [20]

Murtugudde et al. 2000), an Indian-Ocean coupled ocean-atmosphere climate mode that peaks in fall, as discussed in the introduction. This is further demonstrated in Figs. 10c and 10d, which display regression maps of interannual anomalies of OCD, TCD, SST, and winds onto the boreal fall DMI. The resulting patterns, representing the typical anomalies associated with a positive IOD phase, are strikingly similar to those displayed in Figs. 10a and 10b (pattern correlation of ~0.85). This highlights the strong link between the IOD events and the WCI fall oxycline year-to-year variations. We further examine the relationship between the WCI OCD and the IOD in Fig. 11a, which displays time series of fall OCD interannual anomalies and the fall DMI (computed from both modeled and observed SST, the correlation between them being 0.94). Consistent with the regression map, we find a high correlation between the WCI OCD and the DMI (~0.67/0.62 with modeled and observed DMI respectively).

The influences of positive and negative phases of IOD on the WCI OCD (and TCD, not shown) are however not symmetrical (Fig. 11a): most of the positive IOD events cause a deepening of OCD along WCI (e.g., 1961, 1967, 1994, 1997), while negative IOD can either be associated with a shoaling (e.g. 1996, 1998, 2010) or even a deepening (e.g. 1979-81). To further illustrate this asymmetry, Fig. 12 provides a scatterplot of the fall DMI versus the fall interannual anomalies of OCD off the WCI. This scatterplot confirms that there is an asymmetric impact of positive and negative IODs on the OCD along the WCI. The WCI OCD response to positive IODs is very robust, with all positive IOD events (DMI > 1) except one being systematically associated with a deepening. The WCI response to negative IOD is weaker and much less systematic. As discussed above, negative IOD events (DMI<-1) are generally related to negative OCD anomalies but can also be related to positive OCD anomalies (Fig. 11a). Fig. 13 provides a composite of the temporal evolution of the anomalous OCD and TCD along the WCI along with zonal wind stress variations at the STI for signal associated with positive/negative IOD events. It must be noticed here that time series for negative IOD events has been multiplied by -1 to ease comparison with positive events. Figs. 13a and 13b illustrate again the two to three times weaker response of the WCI OCD for negative compared to positive IOD events. This weaker response is related to slightly weaker zonal wind anomalies at the STI (Fig. 13c) that consequently trigger a weaker coastal Kelvin wave response along WCI and thus weaker WCI TCD/OCD anomalies. It is therefore likely that the weaker and less robust wind signal associated with negative IODs at the STI compared to positive IODs may explain part of the asymmetry seen in Fig. 12. We will discuss the possible causes for this asymmetry in section 4.2.

4 Summary and Discussion

4.1 Summary

The year-to-year variations of coastal hypoxia along the west coast of India (WCI) have been identified by Naqvi et al. (2000, 2009), along with their strong impacts on fisheries and ecosystem. The mechanisms controlling these variations have however not yet been elucidated. The present study offers new insights on the physical controls of coastal hypoxia along the

I. Suresh 26/12/2016 10:31 AM
Deleted: Fig.…igs. 10c and 10d-f… whic[... [21]

I. Suresh 26/12/2016 10:31 AM
Deleted: 11b…2 provides a scatterplot of [... [22]

I. Suresh 26/12/2016 10:31 AM
Deleted: fifteen years ago,

WCI. To that end, we used an eddy-permitting (¼° horizontal resolution), regional Indian Ocean configuration of a coupled physical-biogeochemical model. The simulation spans a period long enough (1960-2012) to allow analyzing the driving mechanisms of interannual variability of oxygen off the WCI. The model accurately reproduces the oxycline and thermocline seasonal cycle off the WCI, with a seasonal upwelling that yields shallowest oxycline/thermocline at the end of the summer monsoon. The modeled and observed offshore climatological seasonal cycles of oxygen match in-situ measurements on the shelf, with a strongest seasonal oxygen deficiency and highest occurrence rate of anoxic events during boreal fall. It is suggested that the upwelling of oxygen-depleted subsurface waters at the shelf break influences the occurrence of anoxic events over the western Indian continental shelf.

The shallow oxycline in fall combines with a large interannual variability at this time of the year to create a window of opportunity for coastal anoxic events. Our model analysis further indicates that there is a tight coupling between the thermocline and oxycline variability in this region at both seasonal and interannual timescales, indicative of a strong physical control of the oxygen variability through vertical advection. Interannual thermocline fluctuations along the WCI are related to basin-scale wind, thermocline and oxycline depth perturbations associated with IOD events, an Indian Ocean coupled ocean-atmosphere climate mode that peaks in fall. Positive IOD events are associated with easterly wind anomalies in the central equatorial Indian Ocean, that extend meridionally up to the southern tip of India. These easterly wind anomalies trigger downwelling coastal Kelvin waves that propagate along the WCI and deepen the thermocline and oxycline in boreal fall, thereby preventing the occurrence of coastal anoxia off the WCI during positive IOD events. Our model results also suggest an asymmetry between the impact of positive and negative IOD events on the WCI oxycline depth. The westerly wind anomalies at the southern tip of India indeed have a smaller amplitude during negative IODs than their easterly counterparts during positive IODs, thus resulting in a weaker and less consistent shoaling of oxycline/thermocline along WCI during negative IOD events.

4.2 Discussion

Previous studies have demonstrated the impact of large-scale climate modes on year-to-year variations of the oxygen deficiencies in coastal hypoxic systems elsewhere in the world ocean. In the Pacific, El Niño conditions lead to intensified oxygenation along the coasts of Peru and Chile as a result of weak upwelling (e.g., Arntz et al., 2006; Gutierrez et al., 2008), while in the Atlantic, the Benguela Niño leads to intensified anoxia along the Namibian shelf (Monteiro et al., 2008). The western continental shelf of India is home to the largest naturally-formed coastal hypoxic system in the world. In this study, we identify, for the first time, the IOD as the major climatic driver of the year-to-year oxycline and thermocline variations offshore to the WCI. Though the IOD has a weaker thermocline depth signature on the west than on the east coast of India, it has stronger societal consequences as it influences the WCI seasonal upwelling that brings suboxic waters very close to the surface during fall. Although the IOD influence on the west Indian coast has never been reported so far, it has regularly been reported in the in the Bay of Bengal. In line with our results, Aparna et al. (2012) indeed showed that IOD events drive

I. Suresh 26/12/2016 10:31 AM
Deleted: oxygen

I. Suresh 26/12/2016 10:31 AM
Deleted: along

I. Suresh 26/12/2016 10:31 AM
Deleted: modelled

I. Suresh 26/12/2016 10:31 AM
Deleted: mainly causes

I. Suresh 26/12/2016 10:31 AM
Deleted: Indian Ocean Dipole (

I. Suresh 26/12/2016 10:31 AM
Deleted:)

I. Suresh 26/12/2016 10:31 AM
Deleted: which

I. Suresh 26/12/2016 10:31 AM
Deleted: STI

I. Suresh 26/12/2016 10:31 AM
Deleted: STI

I. Suresh 26/12/2016 10:31 AM
Deleted: OCD

I. Suresh 26/12/2016 10:31 AM
Deleted: .

I. Suresh 26/12/2016 10:31 AM
Deleted: a

I. Suresh 26/12/2016 10:31 AM
Deleted: along

I. Suresh 26/12/2016 10:31 AM
Deleted: The IOD influence is further shown to be larger for positive than negative IOD events.

strong sea-level and thermocline fluctuations along the rim of the Bay in fall, through coastal Kelvin wave propagation from the equatorial region. Akhil et al. (2016) further demonstrated that this remote forcing also drives anti-clockwise anomalous horizontal currents in fall in the Bay, which in turn leads to large interannual variations of Sea Surface Salinity in the southern Andaman Sea. On the biogeochemical side, Wiggert et al. (2002, 2009) and Currie et al. (2013) demonstrated that IOD events are responsible for large interannual chlorophyll variations in the southeastern Bay of Bengal and at the STI. Finally, the IOD signature found in Arabian Sea in the present study has already been described for the Bay of Bengal in terms of sea-level (Aparna et al., 2012) and chlorophyll (Currie et al., 2013).

The influence of IOD is further shown to be larger for positive than its negative phase. Our results suggest that part of the weaker WCI oxycline depth response during negative IOD may be explained by the weaker windstress anomalies at the STI associated with negative IOD events. This weaker wind amplitude could simply be related to the tendency of negative IOD events to be weaker than their positive counterpart (Saji and Yamagata 2003; Hong et al. 2008; Cai et al. 2013) or to asymmetries in the spatial patterns of winds associated associated with the non-linear response of deep atmospheric convection to SST anomalies of each phase of the IOD. A more precise understanding of this asymmetry would require an in-depth investigation of the processes that control the wind variations at the STI and the thermocline along the WCI in response to positive and negative IOD events.

Our findings partly explain the substantial year-to-year changes in both the duration and intensity of the observed seasonal oxygen deficiency over the western Indian shelf (Naqvi et al., 2009). None of the anoxic events reported by Naqvi et al. (2009) (black stars in Fig. 12) lies on the upper right quadrant of the scatterplot shown in Fig. 12, indicating that positive IODs systematically prevent the occurrence of anoxic events. For instance, the relaxation of anoxic condition in early fall 1997 reported by Naqvi et al. (2009) is in line with the occurrence of very strong positive IOD during that year. Most anoxic events are found in the lower left quadrant, i.e., near neutral or negative IOD conditions and anomalously shallow offshore oxycline. Neutral or negative IOD years are however not necessarily anoxic, indicating that a neutral or negative IOD is a necessary but not a sufficient condition for severe anoxia. A recent study by Gupta et al. (2016) revealed that the oxygen deficiency in 1959 along the WCI was more severe than in 2012, a conclusion consistent with the occurrence of a negative IOD in 1959 and a positive one in 2012. Similarly, in-situ measurements also revealed that subsurface oxygen concentrations were significantly lower at the turn of the 20th century than in the 70's (Naqvi et al., 2009): our simulation exhibit a similar behavior (see Fig. 11a), showing many years with shallower than normal OCD in the later period and systematically deeper than normal OCD during 1970's. The causes for those decadal variations need to be investigated in greater detail.

The ~0.7 correlation between IOD variability and oxycline variations along the WCI implies that ~50% of the interannual oxycline variance is explained by the IOD at this location. This relationship between the IOD and year-to-year variations of seasonal anoxic conditions along the shelf may facilitate advance warning for the possible occurrence of severe anoxic

I. Suresh 26/12/2016 10:31 AM
Deleted: asymmetrical

I. Suresh 26/12/2016 10:31 AM
Deleted: Although our results suggest that part of this asymmetry may be explained by the difference in the strength of winds at STI associated with each phase of the IOD, an in-depth investigation of the processes that control the thermocline along the WCI in response to positive and negative IOD events is required.

I. Suresh 26/12/2016 10:31 AM
Deleted: 11b

I. Suresh 26/12/2016 10:31 AM
Deleted: 11b

events. Recent studies indeed indicate that skillful predictions of mature IOD events in fall can be achieved about one season ahead (e.g. Luo et al., 2007; Wang et al., 2009; Zhao and Hendon 2009; Sooraj et al., 2012) and up to two seasons ahead in the case of large IOD events (Luo et al., 2007, 2008; Shi et al., 2012). Those predictions of IOD events should allow providing a warning about the likelihood of severe anoxic conditions along the WCI during spring or summer. A predicted positive IOD is indeed associated with very low chances of such an anoxic event, while neutral or negative IOD conditions may be associated with the occurrence of such an event.

It must however be kept in mind that other factors are also likely to contribute to the reported interannual fluctuations of hypoxic conditions in this region. Naqvi et al. (2009) for instance suggested that increased productivity due to increased nutrient loading from land associated with anthropogenic activities might have the potential to trigger a shift from natural suboxic to anthropogenic anoxic conditions during recent decades. This hypothesis however cannot explain the relaxation of the intensity of oxygen deficiency in the recent decades. Another contributing factor could be related to changes in local hydrographic variations. For instance, interannual variations of the land runoff along the Western Ghats, local precipitation during summer monsoon or input of Bay of Bengal freshwater during the northeast monsoon (e.g. Jensen et al., 2001) could modulate the upper ocean haline stratification, ventilation of the subsurface waters and hence the subsurface oxygen content along the WCI. Finally, local alongshore wind variations may modulate the intensity of coastal upwelling and hence the amount of oxygen-depleted waters brought to the shelf. The influence of these factors hence requires further investigation.

An obvious limitation of the current study is the spatial resolution of our model (~25 km). While our model has a reasonable representation of the temperature and oxygen seasonal variations in the deep ocean off the shelf break, its spatial resolution is not sufficient to resolve the details of physical processes controlling the upwelling along shelf break (e.g. Huthnance 1995; Allen et al. 2010). For the case of the narrow continental shelf along the west coast of North America, several studies have shown that a minimum horizontal resolution of 10 km is required (Marchesiello et al., 2003; Veneziani et al., 2009). For example, at ¼° resolution our model is eddy-permitting, but not eddy-resolving, and hence does not fully capture oceanic mesoscale eddies, which play an important role for the exchanges between the shelf and the open ocean in upwelling regions (e.g. Marchesiello et al. 2003 Bettencourt et al. 2015; Vergara et al. 2016). Another limitation arises from the absence of tidal forcing in the model, which may play an important role, as strong internal tides can be generated on the shelf break and contribute to enhance the thermocline vertical excursion and mixing, which can both contribute to bring more deep ocean oxygen-deficient water to the shelf (Monteiro et al. 2005).

While our model does not reproduce the details of exchanges between the shelf and open ocean, we have just used it as a proxy of the behaviour of open ocean, off the WCI. Several studies have already pointed towards the influence of offshore oxygen variations in driving the variability of hypoxic conditions along other coastal regions (e.g. Grantham et al. 2004; Helly and Levine, 2004; Arntz et al., 2006; Gutierrez et al., 2008). As was shown in Figs. 6 and 7b, the model and WOA

I. Suresh 26/12/2016 10:31 AM
Deleted: with

I. Suresh 26/12/2016 10:31 AM
Deleted: The present study has some inherent limitations though. The horizontal resolution of the model (1/4°) does not resolve the fine-scale interactions between the shelf and the deep ocean, including the detailed structure of the coastal upwelling. Our model is eddy-permitting, but not really eddy-resolving, and hence does not capture oceanic mesoscale eddies, which play an important role for coastal-offshore exchanges. Increasing the upper-ocean vertical resolution and accounting for WCI runoffs interannual variability (which are climatological in the present setup) may also improve the representation of the upper-ocean stratification, subsurface ventilation and oxygen variability along the WCI.

climatology vertical oxygen distribution agree quite well, both in terms of the oxycline depth and near-surface value. The CaTS data, on the other hand, is representative of what happens much closer to the coast and displays much lower oxygen levels than seen further offshore in WOA and the model. This may of course partially be due to shortcomings in representing physical exchanges between the shelf and open ocean at the current resolution of our model and existing oxygen dataset in the region. But biological processes are also known to be a prominent oxygen consumption factor on the shelf, in particular in the benthic zone where the enhanced concentration of particulate matter above sediments is associated with high oxygen demand (e.g. Cowie, 2005). The crude parameterization of sediments in the model probably does not consume enough oxygen very close to the coast. On the other hand, the good phasing between the oxygen seasonal variability offshore (in the model and WOA) and shelf (CaTS) data (Figs. 7b and 7c) suggests that the offshore variability is probably an important driver of the oxygen content on the shelf. However, a proper representation of benthic biological processes would probably be needed to represent the low oxygen levels very close to the coast (Fig. 7c). Dedicated studies at higher spatial resolution with sensitivity tests on the representation of near-shore biological processes will probably be needed in order to better understand how the representation of near-shore biological processes constrain the coastal oxygen representation.

On the observational front, the current spatio-temporal sampling does not allow building reliable long-term time series of the month-to-month oxygen variations along the shelf and offshore. Despite the establishment of frequent measurements of oxygen profile off Goa since September 1997, the numerous unsampled months (July and August are almost unsampled because of rough weather conditions) and the strong sub-monthly variability prevent a continuous monitoring of oxygen variations along the WCI. A reasonable number of moorings or Argo drifters with oxygen and temperature sensors along the shelf and further offshore would allow a finer description of the oxygen variability, its relationship with temperature and connection with the offshore variations. In order to establish an unequivocal evidence for the shelf-open ocean interactions, future studies should also consider improved observations such as repeated glider transects or triad of moorings (shelf, shelf break and open ocean) monitoring both physical and biogeochemical quantities in this region. Though the present study is focused on the WCI, our Indian Ocean configuration model allows assessing other regions where near-surface hypoxia can occur. Fig. 14 shows the percentage of profiles where oxygen concentrations below 80 µmol.l^{-1} occur within the top 50 m. This threshold is indicative of the limit under which many organisms start to suffer from physiological stress that could ultimately lead to death (Vaquer-Sunyer and Duarte, 2008). This analysis indicates that the coast of Oman can also experience hypoxic conditions as reported in the literature (e.g., Piontovski and Al-Oufi, 2015), although hypoxia along Oman is never as severe as that off WCI (Naqvi et al., 2010b). Fig. 14 indicates that the northwestern Bay of Bengal can also experience near-surface low-level oxygen concentrations, as reported from a series of ship cruise measurements by Sarma et al. (2013). Further examination of the mechanisms driving these hypoxic events reveal that the IOD strongly impacts the oxygen variability in the northwestern Bay of Bengal: positive IOD events generally inducing a shoaling of the oxycline in this region (see Fig. 10c) through upwelling coastal Kelvin wave propagation from the equatorial region. In contrast, the influence of IOD along the Omani coast is almost negligible (Fig. 10c), and oxygen variations here seem to be related to

I. Suresh 26/12/2016 10:31 AM
Deleted: 13

I. Suresh 26/12/2016 10:31 AM
Deleted: along the

I. Suresh 26/12/2016 10:31 AM
Deleted: 13

I. Suresh 26/12/2016 10:31 AM
Deleted: 10d

I. Suresh 26/12/2016 10:31 AM
Deleted: 10d

offshore Ekman pumping (not shown). Further dedicated studies are needed to better understand the oxygen variability in these sensitive regions and their potential impacts on the ecosystem and fisheries.

Acknowledgements

This work is a part of CSIR-funded INDIAS IDEA project. I. Suresh acknowledges financial support from Council of Scientific and Industrial Research, New Delhi and INCOIS/MoES (HOOFS program). V. Parvathi is funded by CSIR under Senior Research Fellowship. We thank CSIR-NIO data centre and Chemical Oceanography Division for making the archived cruise and CaTS data available for the present study. We thank the NEMO-PISCES modeling team. The simulations were performed on HPC Pravah at CSIR-NIO. We thank M. Afroosa for assistance in data processing. M. Lengaigne, C. Ethé, J. Vialard and M. Levy benefited from Institut de Recherche pour le Développement (IRD) funding for their visits to the CSIR-NIO. This is NIO contribution number XXXX.

References

Akhil, V. P., Lengaigne, M., Vialard, J., Durand, F., Keethi, M. G., Chaitanya, A. V. S., Papa, F., de Boyer Montégut, C.: A modelling study of the processes controlling the Bay of Bengal Sea Surface Salinity interannual variability, J. Geophys. Res. Oceans, 121, doi:10.1002/2016JC011662, 2016.

Akhil, V. P., Durand, F., Lengaigne, M., Vialard, J., Keethi, M. G., Gopalakrishna, V. V., Deltel, C., Papa, F., de Boyer Montégut, C.: A modelling study of the processes of surface salinity seasonal cycle in the Bay of Bengal, J. Geophys. Res., 116, 3926-3947, doi:10.1002/2013JC009632, 2014.

Allen, J. I., Aiken, J., Anderson, T. R., Buitenhuis, E., Cornell, S., Geider, R. J., ... & Hardman-Mountford, N. : Marine ecosystem models for earth systems applications: The MarQUEST experience. Journal of Marine Systems, 81(1), 19-33, 2010.

Annamalai, H., Murtugudde, R., Potemra, J., Xie, S. P., Liu, P., Wang, B.: Coupled dynamics over the Indian Ocean: spring initiation of the zonal mode, Deep Sea Res II 50:2305–2330, 2003.

Aparna, S. G., McCreary, J. P., Shankar, D., and Vinayachandran, P. N.: Signatures of Indian ocean dipole and El Niño-Southern oscillation events in sea level variations in the Bay of Bengal, J. Geophys. Res., 117, C10012, doi:10.1029/2012JC008055, 2012.

Arntz, W. E., Gallardo, V. A., Gutierrez, D., Isla, E., Levin, L. A., Mendo, J., Neira, C., Rowe, G. T., Tarazona, J., and Wolff, M.: El Niño and similar perturbation effects on the benthos of the Humboldt, California, and Benguela Current upwelling ecosystems, Adv. Geosci., 6, 243–265, 2006.

I. Suresh 26/12/2016 10:31 AM
Deleted: Submitted to JGR Oceans

I. Suresh 26/12/2016 10:31 AM
Moved down [5]: Arntz, W. E., Gallardo, V. A., Gutierrez, D., Isla, E., Levin, L. A., Mendo, J., Neira, C., Rowe, G. T., Tarazona, J., and Wolf

I. Suresh 26/12/2016 10:31 AM
Moved down [6]: Wolff, M.: El Niño and similar perturbation effects on the benthos of the Humboldt, California, and Benguela Current upwelling ecosystems, Adv. Geosci., 6, 243

I. Suresh 26/12/2016 10:31 AM
Moved down [7]: Geosci., 6, 243–265, 2006.

I. Suresh 26/12/2016 10:31 AM
Moved (insertion) [5]

I. Suresh 26/12/2016 10:31 AM
Moved (insertion) [6]

I. Suresh 26/12/2016 10:31 AM
Moved (insertion) [7]

Aumont, O. and Bopp, L.: Globalizing results from ocean in situ iron fertilization studies, Global Biogeochem. Cy., 20, GB2017, doi:10.1029/2005GB002591, 2006.

Aumont, O., Ethé, C., Tagliabue, A., Bopp, L., and Gehlen, M.: PISCES-v2: an ocean biogeochemical model for carbon and ecosystem studies. Geoscientific Model Development, 8(8), 2465-2513, 2015.

Banse, K.: On upwelling and bottom-trawling off the south west coast of India, J. Mar. Biol. Assoc. India, 1, 33–49, 1959.

Barnier, B., Madec, G., Penduff, T., Molines, J., Treguier, A., Sommer, J. L., Beckmann, A., Biastoch, A., Boning, C., Dengg, J.,Derval, C., Durand, E., Gulev, S., Remy, E., Talandier, C., Theetten, S., Maltrud, M., McClean, J., and Cuevas, B. D.: Impact of partial steps and momentum advection schemes in a global ocean circulation model at eddy permitting resolution, Ocean Dynam.,56, 543–567, doi:10.1007/s10236-006-0082-1, 2006.

Bettencourt, J. H., López, C., Hernández-García, E., et al: Boundaries of the Peruvian oxygen minimum zone shaped by coherent mesoscale dynamics. Nature Geoscience 8:937–940. doi: 10.1038/ngeo2570, 2015.

Boyer, T. P., Antonov, J. I., Baranova, O. K., Coleman, C., Garcia, H. E., Grodsky, A., Johnson, D. R., Locarnini, R. A., Mishonov, A. V., O'Brien, T. D., Paver, C. R., Reagan, J. R., Seidov, D., Smolyar, I. V., and Zweng, M. M.: World Ocean Database 2013, NOAA Atlas NESDIS 72, S. Levitus, Ed., A. Mishonov, Technical Ed.; Silver Spring, MD, 209 pp., 2013.

Brodeau, L., Barnier, B., Penduff, T., Treguier, A.-M., and Gulev, S.: An ERA40 based atmospheric forcing for global ocean circulation models, Ocean Model., 31, 88–104, doi:10.1016/j.ocemod.2009.10.005, 2009.

Cai, W., Zheng, X. T., Weller, E., Collins, M., Cowan, T., Lengaigne, M., ... & Yamagata, T. (2013). Projected response of the Indian Ocean Dipole to greenhouse warming. Nature Geoscience, 6(12), 999-1007.

Carruthers, J. N., Gogate, S. S., Naidu, J. R., and Laevastu, T.: Shoreward upslope of the layer of minimum oxygen off Bombay: Its influence on marine biology, especially fisheries, Nature, 183,1084–1087, 1959.

Cowie G.L., The biogeochemistry of Arabian Sea surficial sediments: a review of recent studies, Prog. Oceanogr., 65, pp. 260–289, 2005.

Currie, J., Lengaigne, M., Vialard, J., Kaplan, D., Aumont, O., Maury, O.: Indian Ocean Dipole and El Niño/Southern Oscillation impacts on regional chlorophyll anomalies in the Indian Ocean. Biogeosciences 10:5841–5888, 2013.

Diaz, R. J. and Rosenberg, R.: Spreading dead zones and consequences for marine ecosystems., Science, 321, 26–29, 2008.

Dussin, R., Treguier A.-M., Molines, J. M., Barnier, B., Penduff, T., Brodeau, L., Madec, G.: Definition of the interannual experiment ORCA025-B83, 1958–2007, LPO Report 902, 2009.

Eilola, K., Meier, H. E. M., and Almroth, E.: On the dynamics of oxygen, phosphorus and cyanobacteria in the Baltic Sea: A model study, J. Marine Syst., 75, 163–184, doi:10.1016/j.jmarsys.2008.08.009, 2009.

Fukumori, I., Raghunath, R., and Fu, L.: Nature of global large scale sea level variability in relation to atmospheric forcing: A modeling study, J. Geophys. Res., 103(C3), 5493-5512, 1998.

I. Suresh 26/12/2016 10:31 AM
Moved down [8]: Brodeau, L., Barnier, B., Penduff, T., Treguier, A.-M., and Gulev, S.: An ERA40 based atmospheric forcing for global ocean circulation models, Ocean Model., 31, 88–104, doi:10.1016/j.ocemod.2009.10.005, 2009.

I. Suresh 26/12/2016 10:31 AM
Moved (insertion) [8]

I. Suresh 26/12/2016 2:22 PM
Formatted: Font:Not Italic

I. Suresh 26/12/2016 2:22 PM
Formatted: Font:Not Italic

I. Suresh 26/12/2016 10:31 AM
Moved (insertion) [9]

I. Suresh 26/12/2016 10:31 AM
Moved up [9]: Carruthers, J. N., Gogate, S. S., Naidu, J. R., and Laevastu, T.: Shoreward upslope of the layer of minimum oxygen off Bombay: Its influence on marine biology, especially fisheries, Nature, 183,1084–1087, 1959.

Geider, R. J., MacIntyre, H. L., and Kana, T. M.: A dynamic regulatory model of phytoplanktonic acclimation to light, nutrients, and temperature, Limnol. Oceanogr., 43, 679–694, 1998.

Grantham, B. A., Chan, F., Nielsen, K. J., et al : Upwelling-driven nearshore hypoxia signals ecosystem and oceanographic changes in the northeast Pacific. Nature 429:749–754. doi: 10.1038/nature02605, 2004.

Gregoire, M. and Friedrich, J.: Nitrogen budget of the northwestern Black Sea shelf as inferred from modeling studies and in-situ benthic measurements, Mar. Ecol.-Prog. Ser., 270, 15–39, 2004.

Gupta, G. V. M., Sudheesh, V., Sudharma, K. V., Saravanane, N., Dhanya,V., Dhanya, K. R., Lakshmi, G., Sudhakar, M., and Naqvi, S. W. A.: Evolution to decay of upwelling and associated biogeochemistry over the southeastern Arabian Sea shelf, J. Geophys. Res. Biogeosci., 121,159-175, doi:10.1002/2015JG003163, 2016.

Gutierrez, D., Enriquez, E., Purca, S., Quipuzcoa, L., Marquina, R., Flores, G., and Graco, M.: Oxygenation episodes on the continental shelf of central Peru: Remote forcing and benthic ecosystem response, Prog. Oceanogr., 79, 177–189, 2008.

Helly, J. J. and Levin, L. A.: Global distribution of naturally occurring marine hypoxia on continental margins, Deep-Sea Res. I, 51, 1159–1168, 2004.

Hetland, R. and DiMarco, S.: How does the character of oxygen demand control the structure of hypoxia on the Texas-Louisiana continental shelf?, J. Mar. Syst., 70, 49–62, doi:10.1016/j.jmarsys.2007.03.002, 2008.

Jensen, T. G.: Arabian Sea and Bay of Bengal exchange of salt and tracers in an ocean model. Geophys. Res. Lett., 28(20), 3967–3970, doi:10.1029/2001GL013422, 2001.

John M. Huthnance, Circulation, exchange and water masses at the ocean margin: the role of physical processes at the shelf edge, Progress in Oceanography, Volume 35, Issue 4 Pages 353-431, ISSN 0079-6611, http://dx.doi.org/10.1016/0079-6611(95)80003-C, 1995.

Keerthi, M.G., Lengaigne, M., Drushka, K., Vialard, J., de Boyer Montégut, C., Pous, S., Levy, M., and Muraleedharan, P. M.: Intraseasonal variability of mixed layer depth in the tropical Indian, Clim. Dyn., doi:10.1007/s00382-015-2721-z, 2015.

Keerthi, M.G., Lengaigne, M., Levy, M., Vialard, J., Parvathi, V., de Boyer Montégut, C., Ethe, C., Aumont, O., Suresh, I., and Muraleedharan, P. M.: Physical control of the interannual variations of the winter chlorophyll bloom in the northern Arabian Sea, Biogeosciences Discuss., doi:10.5194/bg-2016-153, in review, 2016.

Koné, V., Aumont, O., Lévy, M., and Resplandy, L.: Physical and Bio-geochemical controls of the Phytoplankton Seasonal Cycle in the Indian Ocean: a modeling study. in: Wiggert J. D., Hood, R. R., Naqvi, S. W. A., Brink, K. H., and Smith, S. L., 185, 147–166, American Geophysical Union, Washington DC, USA, 2009.

Kortzinger, A., Hedges, J. I., and Quay, P. D.: Redfield ratios revisited: Removing the biasing effect of anthropogenic CO2. Limnol. Oceanogr. 46 : 964–970, 2001

Unknown
Field Code Changed

Krishnakumar, P. K. and Bhat, G. S.: Seasonal and interannual variations of oceanographic conditions off Mangalore coast (Karnataka, India) in the Malabar upwelling system during 1995–2004 and their influences on the pelagic fishery.Fisheries Oceanography, 17 (1). pp. 45-60, 2008.

Large, W. G., Yeager, S. G.: Diurnal to decadal global forcing for ocean and sea-ice models: the data sets and flux climatologies. NCAR/TN-460 STR, 111 pp, 2004.

Lengaigne, M., Menkes, C., Aumont, O., Gorgues, T., Bopp, L., Andre, J. M., Madec, G.: Influence of the oceanic biology on the tropical Pacific climate in a coupled general circulation model. Climate Dynamics 28, 503–516, 2007.

Levy, M., Shankar, D., Andre, J. M., Shenoi S. S. C., Durand, F., de Boyer, C., Montegut, C.: Basinwide seasonal evolution of the Indian Ocean's phytoplankton blooms. J Geophys Res 112:C12014, 2007.

Lee, C. M., Jones, B. H., Brink, K. H., Fischer, A. S.: The upper ocean response to monsoonal forcing in the Arabian Sea: seasonal and spatial variability. Deep Sea Res Part II 47:1177–1226, 2000.

Luo, J. J., Masson, S., Behera, S., and Yamagata, T.: Experimental forecasts of the Indian Ocean dipole using a coupled OAGCM. J. Climate, 20, 2178–2190, 2007.

Luo, J. J., Behera, S., Masumoto, Y., Sakuma, H., and Yamagata, T.: Successful prediction of the consecutive IOD in 2006 and 2007, Geophys. Res. Lett., 35, L14S02, doi:10.1029/2007GL032793, 2008.

Madec, G.: NEMO, the ocean engine, Note du Pole de modelisation, Institut Pierre-Simon Laplace (IPSL), France, No 27 ISSN No 1288–1619, available at: "http://www.nemo-ocean.eu/About-"www.nemo-ocean.eu/About-NEMO/Reference-manuals, 2008.

Madhupratap, M., Kumar, S. P., Bhattathiri, P. M. A., Kumar, M. D., Raghukumar, S., Nair, K. K. C., and Ramaiah, N.: Mechanism of the biological response to winter cooling in the northeastern Arabian Sea, Nature, 384, 549–552, 1996.

Maya, M. V., Karapurkar, S. G., Naik, H., Roy, R., Shenoy, D. M., and Naqvi, S. W. A.: Intra-annual variability of carbon and nitrogen stable isotopes in suspended organic matter in waters of the western continental shelf of India. Biogeosciences, 8, 3441–3456, doi:10.5194/bg-8-3441-2011, 2011.

McCreary, J. P., Kundu, P. K., and Molinari, R. L.: A numerical investigation of dynamics, thermodynamics and mixed-layer processes in the Indian Ocean, Progr. Oceanogr., 31, 181–244,doi:10.1016/0079-6611(93)90002-U, 1993.

McCreary, J.P., W. Han, D. Shankar, and S.R. Shetye, Dynamics of the East India Coastal Current, 2, Numerical solutions, J. Geophys. Res., 101, 13,993-14,010, 1996.

McCreary, J. P., Yu, Z., Hood, R., Vinaychandran, P. N., Furue, R., Ishida, A., and Richards, K.: Dynamics of the Indian-Ocean oxygen minimum zones, Progr. Oceanogr., 2013.

Middelburg, J. J., Soetaert, K., Herman, P. M., & Heip, C. H.: Denitrification in marine sediments: A model study. Global Biogeochemical Cycles, 10(4), 661-673, 1996.

I. Suresh 26/12/2016 10:31 AM
Deleted: Yu, Z., Hood, R., Vinaychandran, P. N., Furue, R., Ishida, A.,

I. Suresh 26/12/2016 10:31 AM
Deleted: Richards, K.:

I. Suresh 26/12/2016 10:31 AM
Deleted: Indian- . Ocean oxygen minimum zones, Progr. Oceanogr., 2013.

I. Suresh 26/12/2016 2:22 PM
Formatted: Font:Not Italic

I. Suresh 26/12/2016 2:22 PM
Formatted: Font:Not Italic

Monteiro, P. M. S., Van der Plas, A. K., Melice, J.-L., and Florenchie, P.: Interannual hypoxia variability in a coastal upwelling system: Ocean–shelf exchange, climate and ecosystem-state implications. Deep-Sea Res. Pt. I, 435–450, 2008.

Morales, C. E., Hormazabal, S.E., and Blanco, J. L.: Interannual variability in the mesoscale distribution of the depth of the upper boundary of the oxygen minimum layer off northern Chile (18-24S): implications for the pelagic system and biogeochemical cycling. Journal of Marine Research, 57, pp. 909–932, 1999.

Morrison, J. M., Codispoti, L. A., Smith, S. L., Wishner, K., Flagg, C., Gardner, W. D., Gaurin, S., Naqvi, S. W. A., Manghnani, V., Prosperie, L., and Gundersen, J. S.: The oxygen minimum zone in the Arabian Sea during 1995 - overall seasonal and geographic patterns, and relationship to oxygen gradients, Deep-Sea Res. Pt.II, 46, 1903–1931, doi:10.1016/S0967-0645(99)00048-X, 1999.

Murtugudde, R., McCreary, J. P., and Busalacchi, A. J.: Oceanic processes associated with anomalous events in the Indian Ocean with relevance to 1997–1998, J. Geophys. Res., 105, 3295–3306, 2000.

Naqvi, S.W.A.: Some aspects of the oxygen-deficient conditions and denitrification in the Arabian Sea, J. Mar. Res., 45, 1049-1072, 1987.

Naqvi, S. W. A, Naik, H., Jayakumar, D. A., Pratihary, A. K., Narvenkar, G., Kurian, S., Agnihotri, R., Shailaja, M. S., and Narvenkar, P. V.: Seasonal anoxia over the Western Indian continental shelf, Geophysical Monograph Series, 185,10.1029/2008GM000745, 2009.

Naqvi, S. W. A., Jayakumar, D. A., Narvekar, P. V., Naik, H., Sarma, V.V. S. S., D'Souza, W., Joseph, S., and George, M. D.: Increased narine production of N2O due to intensifying anoxia on the Indian continental shelf, Nature, 408, 346-349, 2000.

Naqvi, S. W. A., Bange, H. W., Farías, L., Monteiro, P. M. S., Scranton, M. I., and Zhang, J.: Marine hypoxia/anoxia as a source of CH_4 and N_2O, Biogeosciences, 7, 2159-2190, doi:10.5194/bg-7-2159-2010, 2010a.

Naqvi, S. W. A., Moffett, J. W., Gauns, M. U., Narvekar, P. V., Pratihary, A. K., Naik, H., Shenoy, D. M., Jayakumar, D. A., Goepfert, T. J., Patra, P. K., Al-Azri, A., and Ahmed, S. I.: The Arabian Sea as a high-nutrient, low-chlorophyll region during the late Southwest Monsoon, Biogeosciences, 7, 2091–2100, 2010, doi:10.5194/bg-7-2091, 2010b.

Naqvi, S. W. A., Naik, H., Pratihary, A. K., D'Souza, W., Narvekar, P. V., Jayakumar, D. A., Devol, A. H., Yoshinari, T., and Saino, T.: Coastal versus open-ocean denitrification in the Arabian Sea, Biogeosciences, 3, 621–633, doi:10.5194/bg-3-621-2006, 2006.

Nisha, K., Lengaigne, M., Gopalakrishna, V. V., Vialard, J., Pous, S., Peter, A-C., Durand, F., Naik, S.: Processes of summer intraseasonal sea surface temperature variability along the coasts of India, Ocean Dynamics, 63, 329-346, 2013.

Pena, M. A., Katsev, S., Oguz, T., Gilbert, D.: Modeling dissolved oxygen dynamics and hypoxia Biogeosciences, 7 (3), pp. 933–957, 2010.

Piontkovski, S. A., and H.S. AL-Oufi: The Omani shelf hypoxia and the warming Arabian Sea, International Journal of Environmental Studies, doi:10.1080/00207233.2015.1012361, 2015.

I. Suresh 26/12/2016 10:31 AM

Deleted: Pillai, V. N., Pillai, V. K., Gopinathan, C. P., and Nandakumar, A.: Seasonal variations in the physical, chemical and biologicalcharacteristics of the eastern Arabian Sea, J. mar. biol. Ass. India, 42 (1&2) : 1 – 20, 2000.

Praveen Kumar B., Vialard, J., Lengaigne, M., Murty, V. S. N., Foltz, G., McPhaden, M. J., Pous, S., and de Boyer Montégut, C.: Processes of interannual mixed layer temperature variability in the Thermocline Ridge of the Indian Ocean, Clim. Dyn., 43, 2377-2397, 2014.

Resplandy, L., Levy, M., Madec, G., Pous, S., Aumont, O., and Kumar, D.: Contribution of mesoscale processes to nutrient budgets in the Arabian Sea, J. Geophys. Res., 116, C11007, doi:10.1029/2011JC007006, 2011.

Resplandy, L., Lévy, M., Bopp, L., Echevin, V., Pous, S., Sarma, V. V. S. S., and Kumar, D.: Controlling factors of the oxygen balance in the Arabian Sea's OMZ, Biogeosciences, 9, 5095–5109, doi:10.5194/bg-9-5095-2012, 2012.

Resplandy, L., Vialard, J., Lévy, M., Aumont, O., and Dandonneau. Y. : Seasonal and intraseasonal biogeochemical variability in the thermocline ridge of the southern tropical Indian Ocean,J. Geophys. Res.,114, C07024,doi:10.1029/2008JC005246, 2009.

Saji, N. H., Goswami, B. N., Vinayachandran, P. N., Yamagata, T.: A dipole mode in the tropical Indian Ocean. Nature 401:360–363, 1999.

Saji, N. H., & Yamagata, T.: Possible impacts of Indian Ocean dipole mode events on global climate. Climate Research, 25(2), 151-169, 2003.

Sarma, V. V. S. S.: An evaluation of physical and biogeochemical processes regulating perennial suboxic conditions in the water column of the Arabian Sea, Global Biogeochem. Cy., 16, 1082, doi:10.1029/2001GB001461, 2002.

Sarma, V. V. S. S., Sridevi, B., Maneesha, K., Sridevi, T., Naidu, S.A., et al.: Impact of atmospheric and physical forcings on biogeochemical cycling of dissolved oxygen and nutrients in the coastal Bay of Bengal. J. Oceanogr., 2013.

Satya Prakash, Prince Prakash and Ravichandran, M.: Can oxycline depth be estimated using sea level anomaly (SLA) in the northern Indian Ocean?, Remote Sensing Letters, 4:11, 1097-1106, DOI: 10.1080/2150704X.2013.842284, 2013.

Schott, F., and J. P. McCreary.: The monsoon circulation ofthe Indian Ocean, Prog. Oceanogr., 51, 1 – 123, 2001

Shetye, S. R., Gouveia, A. D., Shenoi, S. S. C., Sundar, D., Michael, G. S., Almeida, A. M., and Santanam, K.: Hydrography and circulation off the West coast of India during the Southwest monsoon 1987, J. Mar. Res., 48, 359–378, 1990.

Shetye, S. R.: West India Coastal Current and Lakshadweep high/low. Sadhana, 23, 637– 651, 1998

Shi, L., Hendon, H. H., Alves, O., Luo, J–J., Balmaseda, M. and Anderson, D.: How predictable is the Indian Ocean Dipole? Mon. Weather Rev., 140:3867–3884, 2012.

Smitha, B. R., Sanjeevan, V. N., Vimalkumar, K. G., Revichandran, C.: On the upwelling off the southern tip and along the west coast of India, J. Coast. Res., 24(3):95-102, 2008.

Sooraj, K. P., Annamalai, H., Kumar, A., and Wang, H.: A comprehensive assessment of CFS seasonal forecast over the tropics. Wea. Forecasting, 27, 3–27, 2012.

Suresh, I., Vialard, J., Izumo, T., Lengaigne, M., Han, W., McCreary, J., Muraleedharan, P.M.: Dominant role of winds near Sri Lanka in driving seasonal sea-level variations along the west Indian coast, Geophys.Res. Lett., 43,7028–7035, doi:10.1002/2016GL069976, 2016.

I. Suresh 26/12/2016 2:22 PM
Formatted: Font:Not Italic

I. Suresh 26/12/2016 2:22 PM
Formatted: Font:Not Italic

I. Suresh 26/12/2016 2:22 PM
Formatted: Font:Not Italic

I. Suresh 26/12/2016 10:31 AM
Deleted: Shankar, D., Vinayachandran, P. N

I. Suresh 26/12/2016 10:31 AM
Deleted: Unnikrishnan, A. S

I. Suresh 26/12/2016 10:31 AM
Deleted: currents in the north

I. Suresh 26/12/2016 10:31 AM
Deleted: 52, 63–120, 2002.

I. Suresh 26/12/2016 10:31 AM
Deleted: (sumbitted to GRL), 2016.

Takahashi, T., Broecker, W. S., and Langer, S.: Redfield ratio based on chemical data from isopycnal surfaces, J. Geophys. Res., 90,6907–6924, 1985.

Treguier, A.M., Barnier, B., de Miranda, A. P., Molines, J. M., Grima, N., Imbard, M., Madec, G., Messager, C., Reynaud, T. and Michel, S.: An eddy-permitting model of the Atlantic circulation: Evaluating open boundary conditions, J. Geophys. Res., 106, C10, 22,115-22,129, 2001.

Uppala, S. M., KÅllberg, P. W., Simmons, A. J., Andrae, U., Bechtold, V. D. C., Fiorino, M., Gibson, J. K., Haseler, J., Hernandez, A., Kelly, G. A., Li, X., Onogi, K., Saarinen, S., Sokka, N., Allan, R., Andersson, E., Arpe, K., Balmaseda, M., Beljaars, A., van de Berg, L., Bidlot, J., Bormann, N., Caires, S., Chevallier, F., Dethof, A., Dragosavac, M., Fisher, M., Fuentes, M., Hagemann, S., Holm, E., Hoskins, B., Isaksen, L., Janssen, P., Jenne, R., McNally, A., Mahfouf, J.-F., Morcrette, J.-J., Rayner, N., Saunders, R., Simon, P., Sterl, A., Trenberth, K., Untch, A., Vasiljevic, D., Viterbo, P., and Woollen, J.: The ERA-40 re-analysis, Q. J. Roy. Meteor. Soc., 131, 2961–3012, 2005.

Valcke, S.: The OASIS3 coupler: A European climate modelling community software, Geosci. Model Dev., 6(2), 373–388, doi:10.5194/ gmd-6-373-2013, 2013.

Vaquer-Sunyer, R., Duarte, C.M.: Thresholds of hypoxia for marine biodiversity. Proc. Natl. Acad. Sci. 105, 15452–15457, 2008.

Veneziani, M., Edwards, C.A., and Moore, A.M.: A central California coastal ocean modeling study: 2. Adjoint sensitivities to local and remote forcing mechanisms, J. Geophys. Res., 114, C04020, doi:10.1029/2008JC004775, 2009.

Vergara, O., Dewitte, B., Montes, I., Garçon, V., Ramos, M., Paulmier, A., and Pizarro, O.: Seasonal variability of the oxygen minimum zone off Peru in a high-resolution regional coupled model, Biogeosciences, 13, 4389-4410, doi:10.5194/bg-13-4389-2016, 2016.

Vialard, J., Drushka, K., Bellenger, H., Lengaigne, M., Pous, S., Duvel, J-P.: Understanding Madden–Julian-induced sea surface temperature variations in the North Western Australian Basin. Clim Dyn. doi:10.1007/s00382-012-1541-7, 2013.

Wang, L. and Justic, D.: A modeling study of the physical processes affecting the development of seasonal hypoxia over the inner Louisiana-Texas shelf: Circulation and stratification, Cont.Shelf Res., 29, 1464–1476, 2009.

Webster, P. J., Moore, A. M., Loschnigg, J. P., Leben, R. R.: Coupled ocean atmosphere dynamics in the Indian Ocean during 1997-98.Nature 401:356–360, 1999.

Wiggert, J. D., Murtugudde, R., and McClain, C. R.: Processes controlling interannual variations in wintertime (northeast monsoon) primary productivity in the central Arabian Sea, Deep Sea Res., Part II, 47,2319 – 2343, 2002.

Wiggert, J. D., Hood, R., Banse, K., and Kindle, J.: Monsoon driven biogeochemical processes in the Arabian Sea, Progr. Oceanogr., 65, 176–213, doi:10.1016/j.pocean.2005.03.008, theArabian Sea of the 1990s: New Biogeochemical Understanding, 2005.

I. Suresh 26/12/2016 2:22 PM
Formatted: No underline, Font color: Auto

Wiggert, J. D., Vialard, J., and Behrenfeld, M. J.: Basinwide modification of dynamical and biogeochemical processes by the positive phase of the Indian Ocean Dipole during the SeaWiFS era, in: Indian Ocean Biogeochemical Processes and Ecological Variability, vol. 185, edited by: J. D. Wiggert, R. R. Hood, S. Wajih, A. Naqvi, K. H. Brink, and S. L. Smith, p. 350, 2009.

Zhang, Y. C., Rossow, W. B., Lacis, A. A., Oinas, V., Mishchenko, M. I.: Calculation of radiative fluxes from the surface to top of atmosphere based on ISCCP and other global data sets: refinments of the radiative transfer model and the input data. J Geophys Res 109:D19105. doi:10.1029/2003JD004457, 2004.

Zhao, M., and Hendon, H. H.: Representation and prediction of the Indian Ocean dipole in the POAMA seasonal forecast model. Quart. J. Roy. Meteor. Soc., 135, 337–352, 2009.

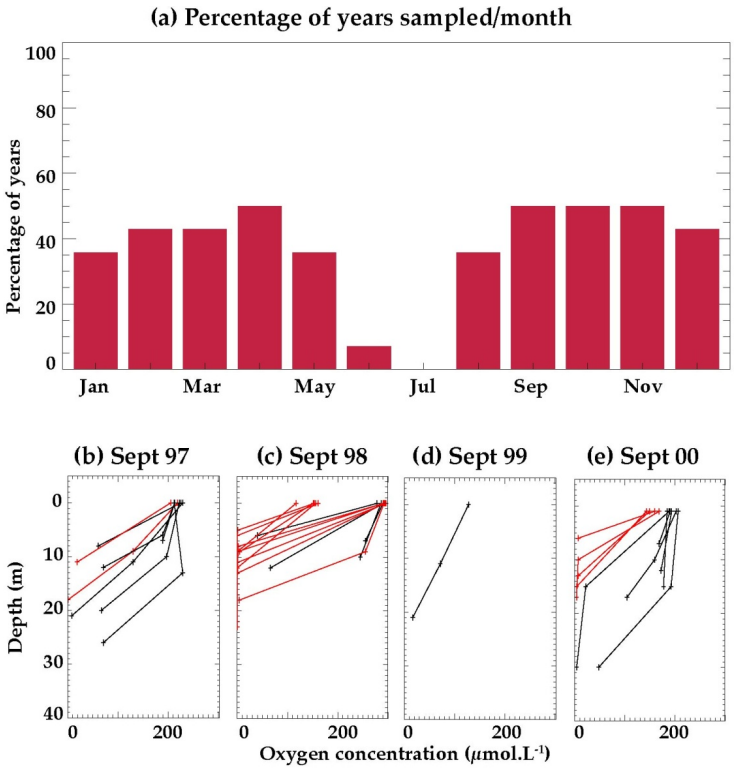

Figure 1. (a) Histogram of the percentage of years sampled for each calendar month over the 1997-2010 period at CaTS station. Vertical oxygen profiles collected at CaTS in September **(b)** 1997, **(c)** 1998, **(d)** 1999 and **(e)** 2000. Profiles with oxygen concentrations below 20 µmol.l^{-1} within the top 20 m of the water column are indicated in red.

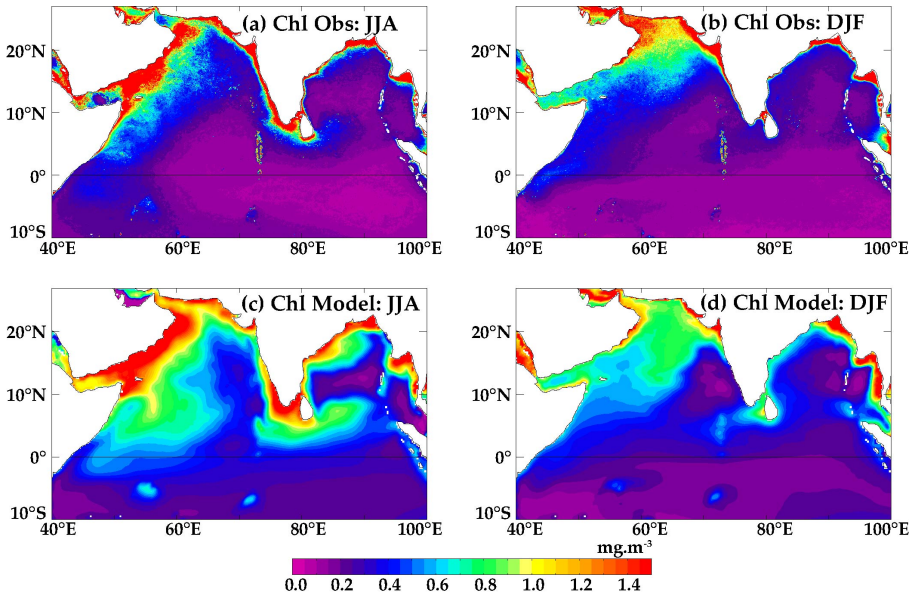

Figure 2. Northern Indian Ocean surface chlorophyll (mg.m^{-3}) climatology for (left) summer (June-August) and (right) winter (December-February) in (top) the ESA satellite product and (bottom) model.

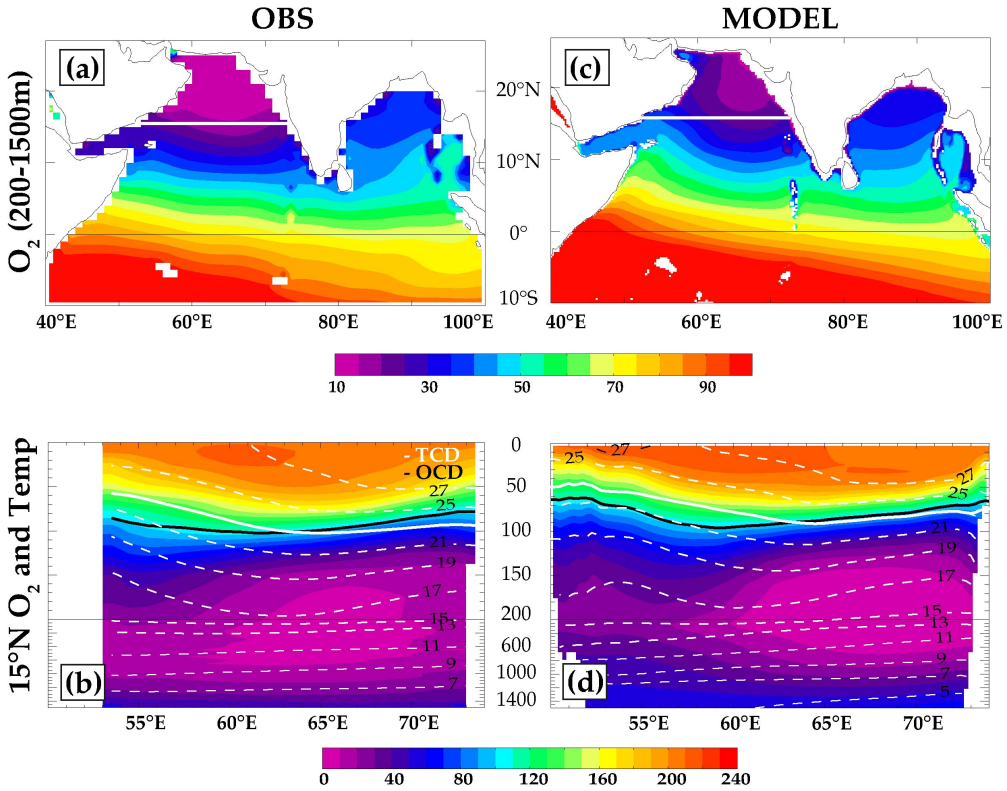

Figure 3. (a) Map of yearly climatological O_2 concentration (µmol.l^{-1}) averaged between 200 and 1500-m depths in the northern Indian Ocean from WOA13. **(b)** the vertical distribution of yearly climatological O_2 (µmol.l^{-1}; shaded) and temperature (^{o}C; dashed white contours with 2°C interval) across East-West section at 15°N (indicated by white line in panels a and c) in the Arabian Sea from WOA13 data. **(c, d)** Same as **(a, b)** but for the model. Depths of 23^{o} C isotherm (white line) and of 100 µmol.l^{-1} isoline (black line) are marked on panels **b** and **d.**

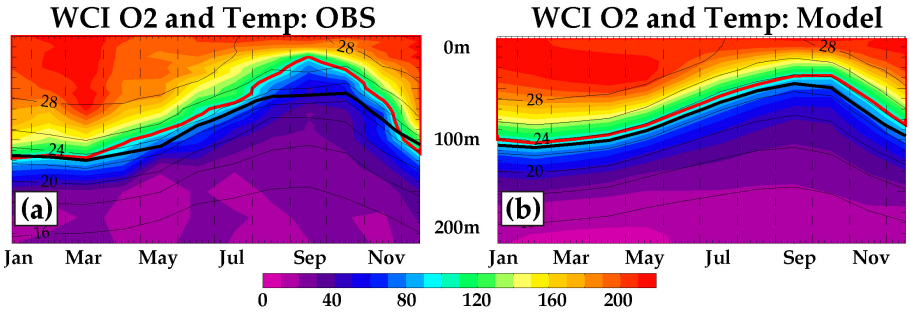

Figure 4. Seasonal evolution of oxygen (µmol.l^{-1}; color shaded) and temperature (^{o}C; thin black contour) vertical profiles averaged over the WCI box (indicated as black frame on Fig. 5) from (a) WOA13 and (b) model . The oxycline and thermocline depths are marked by thick red and black lines respectively in both panels.

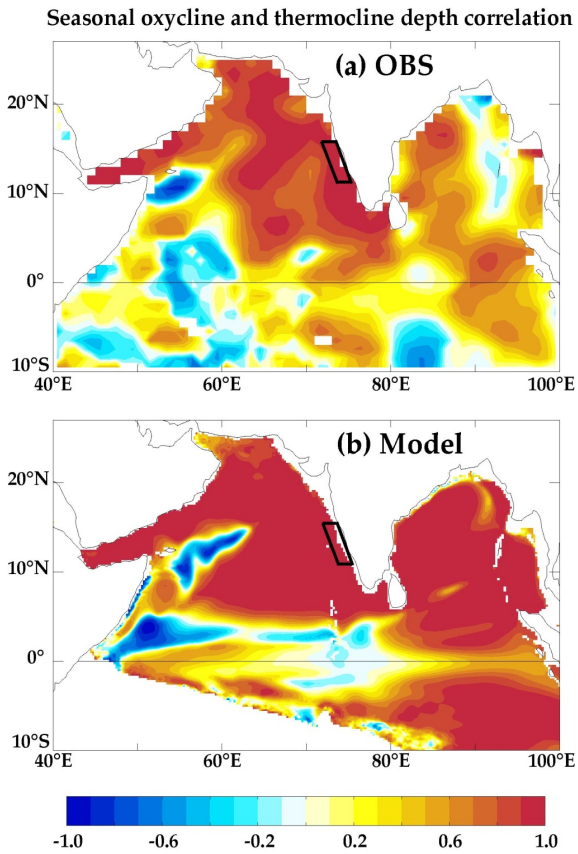

Figure 5. Maps of correlation between the mean seasonal cycle of oxycline and thermocline depths over the northern Indian Ocean from **(a)** WOA13 and **(b)** model. Values are masked when the oxycline could not be defined, i.e., when the oxygen concentration is above 100 µmol.l^{-1} in the entire water column. The WCI box is marked as a black frame on each panel.

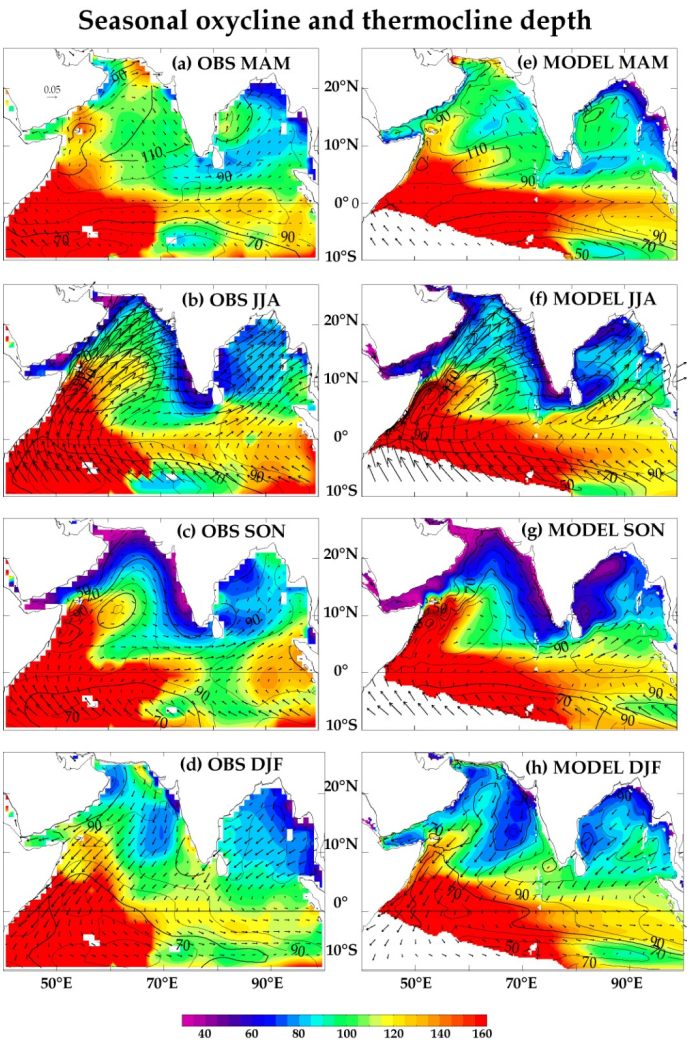

Figure 6. Maps of the seasonal climatology of oxycline (m; shaded) and thermocline depths (m; contours with 10-m interval) from WOA13 during **(a)** March-May, **(b)** June-August, **(c)** September-November and **(d)** December-February. **(e-h)** Same as **(a-d)**, but from the model. Seasonal wind stress ($N.m^{-2}$) patterns from the model forcing field are also shown as vectors on all panels.

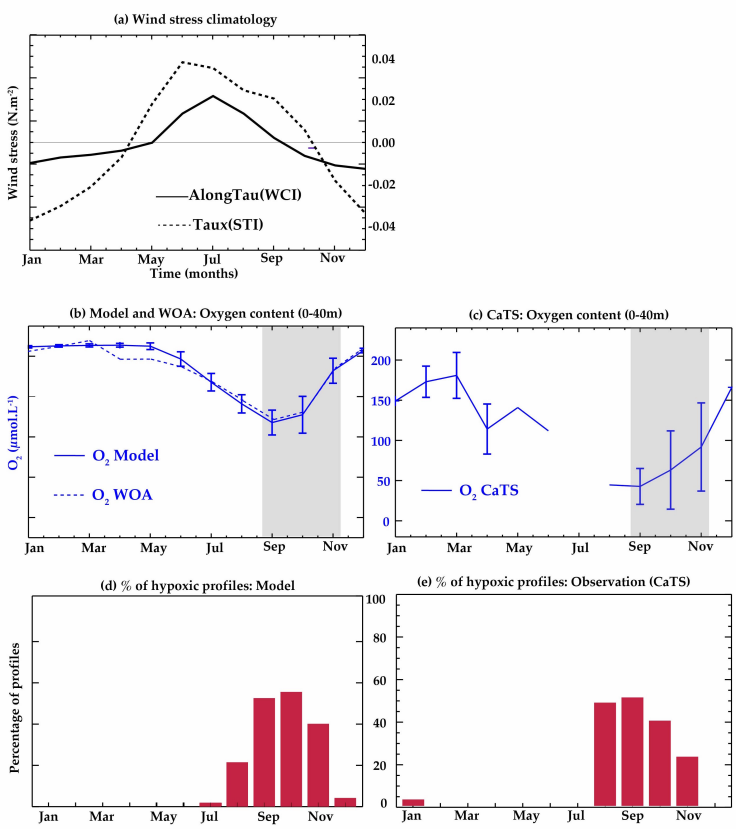

Figure 7. (a) Monthly climatological time series of alongshore wind stress in the WCI box (thick black curve) and zonal wind stress at the southern tip of India (STI; dashed black curve) with positive values denoting the upwelling-favourable winds. Monthly climatological time series of upper ocean (0-40 m depth) averaged oxygen (blue) **(b)** from the model (continuous) and WOA13 (dashed) in the WCI box and **(c)** from the in-situ CaTS data. Vertical bars on panel b and c indicate +/- one standard deviation around the mean value (displayed for CaTS data only when the number of years sampled for a given month exceeds five). Percentage of profiles for each calendar month for which **(d)** oxygen concentrations below 80 µmol.l^{-1} occur within the top 50 m at WCI box in the model and **(e)** oxygen concentrations below 20 µmol.l^{-1} occur within the top 20 m in CaTS data.

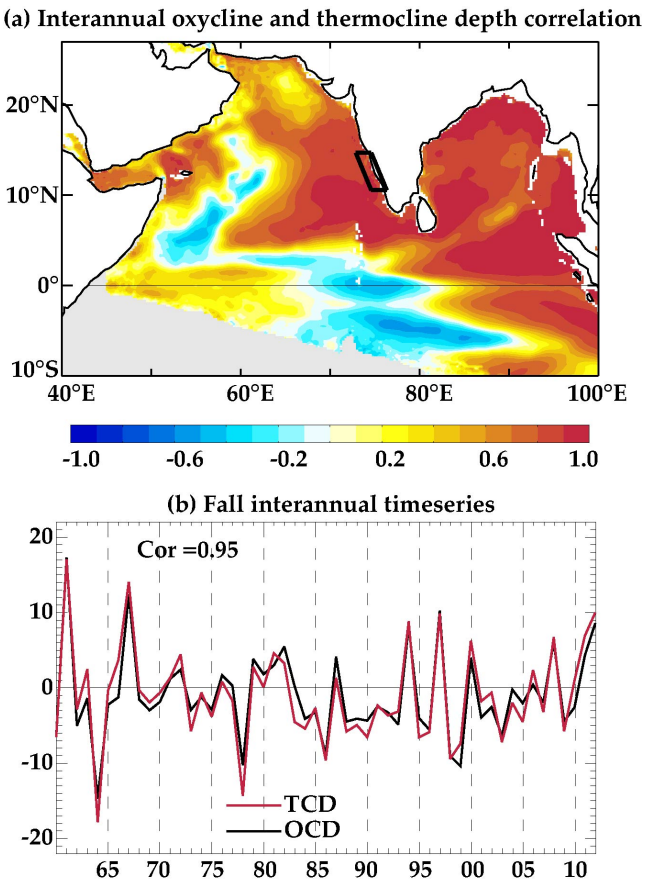

Figure 8. (a) Map of correlation between the modelled oxycline and thermocline depth fall interannual anomalies. **(b)** Time series of fall interannual anomalies of the modeled TCD (m; red line) and OCD (m; black line) averaged over the WCI box (see frame on panel a). On panel (a), values are grey shaded when the oxycline and/or thermocline could not be defined (with their present definition) for more than 20% of the profiles at a given location.

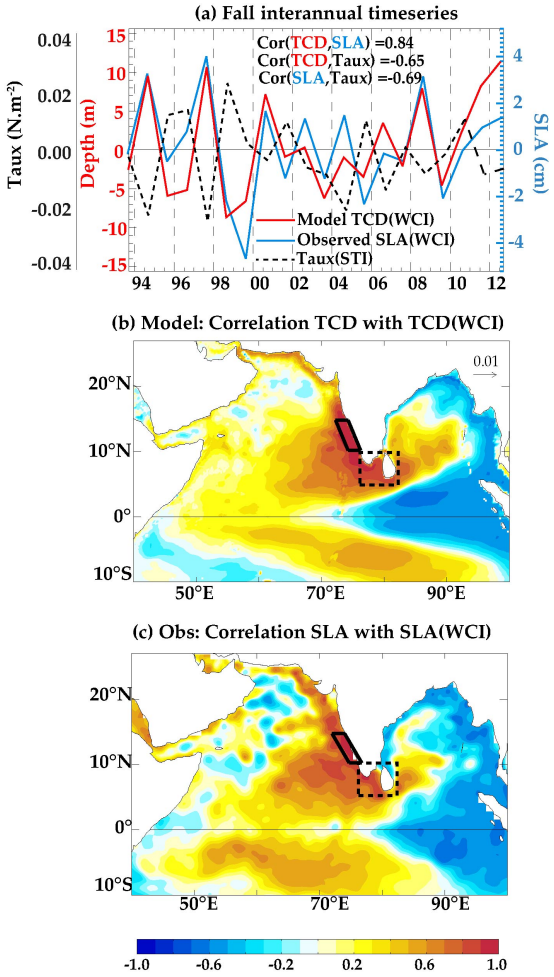

Figure 9. (a) Fall interannual anomalies of the model thermocline depth (red line) and the altimetry-derived sea-level (blue line) averaged over the WCI box (see black frame on panels b and c) along with fall interannual zonal wind stress anomalies (dashed black line) averaged over the STI box (see dashed frame on panels b and c). **(b)** Correlation pattern of fall interannual thermocline anomalies on to that averaged over the WCI box in the model. **(c)** Same as (b) but for altimetry-derived sea-level anomalies.

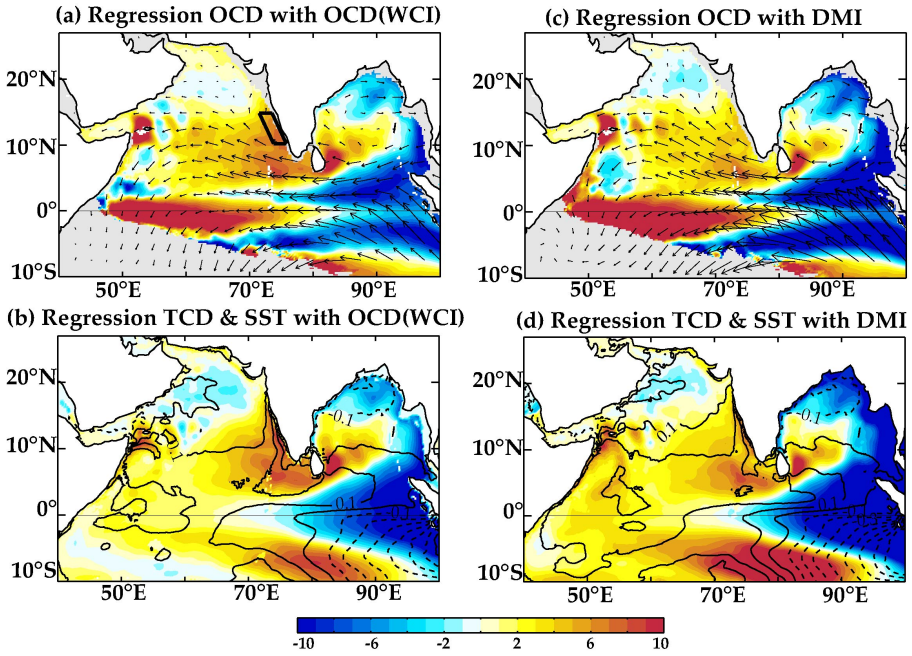

Figure 10. Regression patterns of fall interannual anomalies of modeled **(a)** oxycline (m; shaded) and wind stress ($N.m^{-2}$; vectors), **(b)** thermocline (m; shaded) and SST (^{o}C; contours with 0.1°C interval) onto the fall oxycline interannual anomalies averaged over WCI box normalized by its standard deviation. **(c-d)** Same as **(a-b)** but regressed onto the observed fall DMI index.

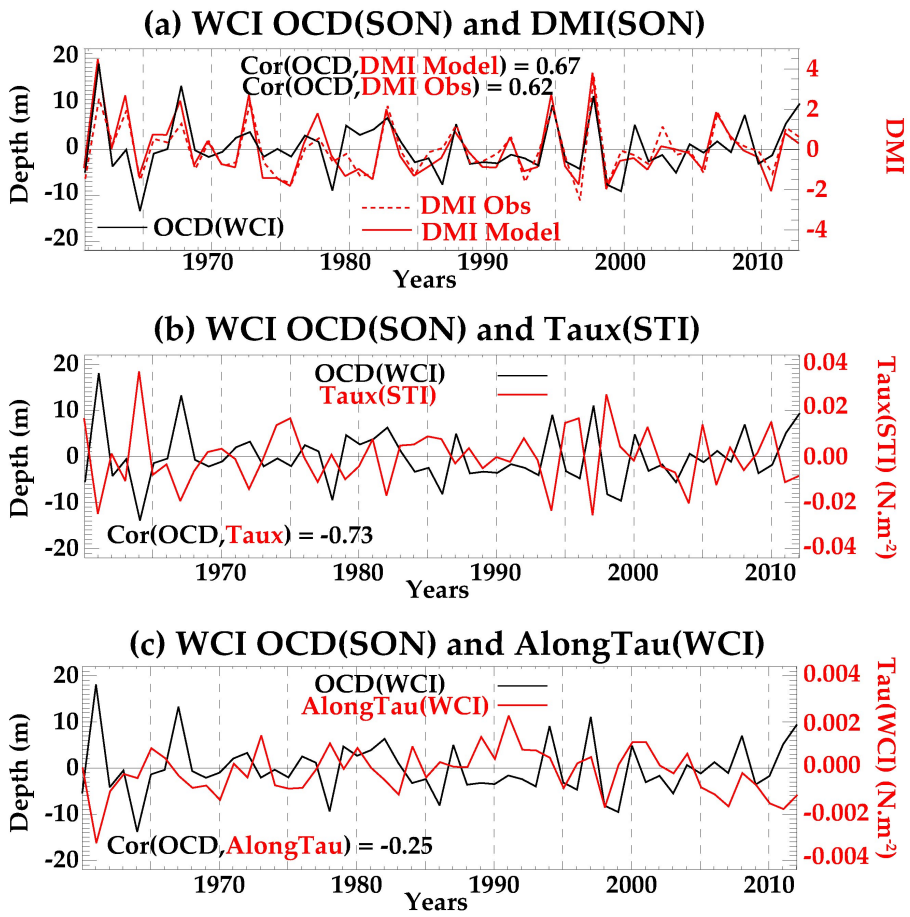

Figure 11. (a) Time series of fall interannual anomalies of modeled oxycline depth (continuous black line) averaged over the WCI box and modeled (continuous red) and observed (dashed red) fall DMI, **(b)** Time series of fall interannual anomalies of modelled oxycline depth averaged over the WCI box (black line) and zonal wind stress averaged over the southern tip of India (red line; STI box shown as dashed frame on Fig. 9b). **(c)** Time series of fall interannual anomalies of modelled oxycline depth (black line) and alongshore wind stress (red line) averaged over the WCI box. Upwelling-favourable winds on panel b and c are positive. Correlation coefficients between the variables are indicated in each panel.

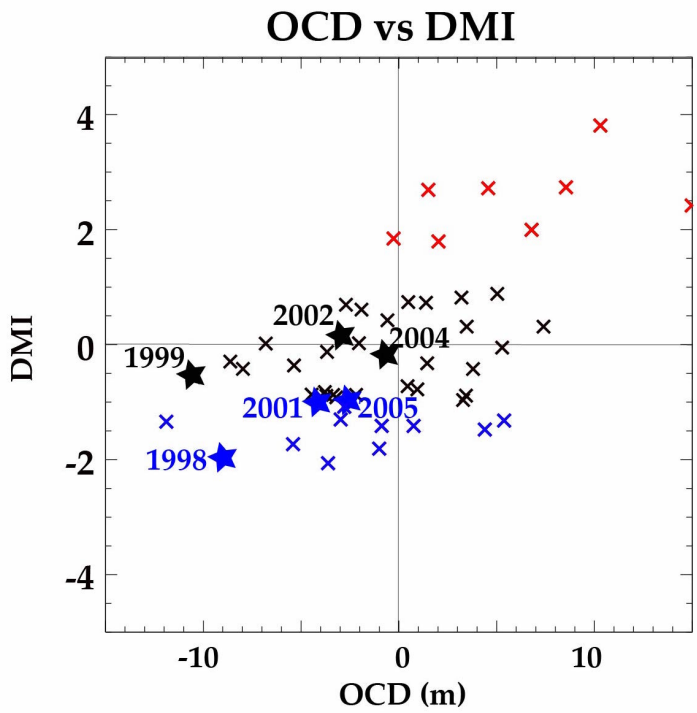

Figure 12. Scatterplot of the fall interannual anomalies of modeled WCI oxycline depth against modeled DMI. Red and blue crosses respectively indicate positive and negative IOD events (defined as events when DMI exceed one standard deviation). Years of anoxic events reported by Naqvi et al. (2009) are marked as stars along with the corresponding years.

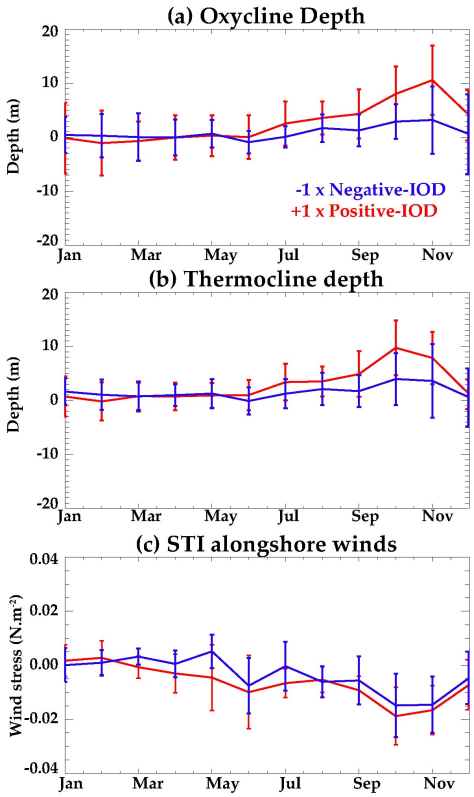

Figure 13. Seasonal evolution of anomalous composites of **(a)** WCI OCD, **(b)** WCI TCD and **(c)** STI zonal wind stress during positive (red) and negative (blue) IOD events. Positive (negative) IODs are defined when the DMI averaged for fall season is greater (lesser) than 1° C. The whiskers indicate the 95% confidence interval on the composited value. Positive IOD events considered in this composite are years 1961, 1963, 1967, 1972, 1977, 1982, 1994, 1997, and 2006 while negative ones are 1964, 1973, 1974, 1975, 1979, 1981, 1984, 1992, 1996, 1998, and 2010. Negative IOD composite time series has been multiplied by -1 to ease comparison with positive events.

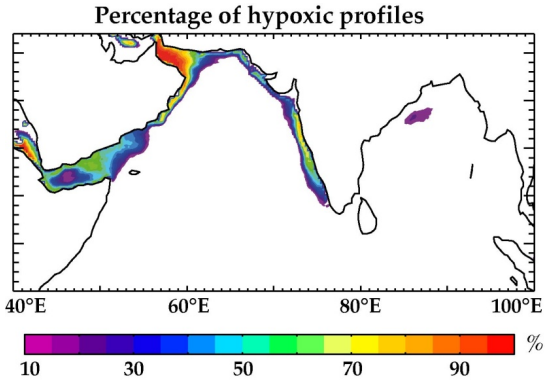

Figure 14. Percentage of occurrence of near-surface hypoxic conditions in the model during fall. Near-surface hypoxic conditions are defined as profiles with oxygen concentration below 80 μmol.l^{-1} (a threshold under which a most large marine organism suffer from stress) in the upper 50 m.